Eur. Phys. J. C 47, 625–641 (2006)
Digital Object Identifier (DOI) 10.1140/epjc/s2006-02596-4

THE EUROPEAN PHYSICAL JOURNAL C

$B \to K^*\ell^+\ell^-$ decay in soft-collinear effective theory

A. Ali[1,a], G. Kramer[2,b], G. Zhu[2,c]

[1] Theory Group, Deutsches Elektronen-Synchrotron DESY, Notkestrasse 85, 22603 Hamburg, Germany
[2] II. Institut für Theoretische Physik, Universität Hamburg, Luruper Chaussee 149, 22761 Hamburg, Germany

Received: 7 March 2006 / Revised version: 20 April 2006 /
Published online: 18 July 2006 –

Abstract. We study the rare B decay $B \to K^*\ell^+\ell^-$ using soft-collinear effective theory (SCET). At leading power in $1/m_b$, a factorization formula is obtained valid to all orders in α_s. For phenomenological application, we calculate the decay amplitude including order α_s corrections, and resum the logarithms by evolving the matching coefficients from the hard scale $\mathcal{O}(m_b)$ down to the scale $\sqrt{m_b\Lambda_h}$. The branching ratio for $B \to K^*\ell^+\ell^-$ is uncertain due to the imprecise knowledge of the soft form factors $\zeta_\perp(q^2)$ and $\zeta_\parallel(q^2)$. Constraining the soft form factor $\zeta_\perp(q^2=0)$ from data on $B \to K^*\gamma$ yields $\zeta_\perp(q^2=0) = 0.32 \pm 0.02$. Using this input, together with the light-cone sum rules to determine the q^2-dependence of $\zeta_\perp(q^2)$ and the other soft form factor $\zeta_\parallel(q^2)$, we estimate the partially integrated branching ratio in the range $1\,\mathrm{GeV}^2 \le q^2 \le 7\,\mathrm{GeV}^2$ to be $(2.92^{+0.67}_{-0.61}) \times 10^{-7}$. We discuss how to reduce the form factor related uncertainty by combining data on $B \to \rho(\to \pi\pi)\ell\nu_\ell$ and $B \to K^*(\to K\pi)\ell^+\ell^-$. The forward-backward asymmetry is less sensitive to the input parameters. In particular, for the zero-point of the forward-backward asymmetry in the standard model, we get $q_0^2 = (4.07^{+0.16}_{-0.13})\mathrm{GeV}^2$. The scale dependence of q_0^2 is discussed in detail.

PACS. 13.25.Hw; 12.39.St; 12.38.Bx

1 Introduction

The electroweak penguin decay $B \to K^*\ell^+\ell^-$ is loop-suppressed in the standard model (SM). It may therefore provide a rigorous test of the SM and also put strong constraints on the flavor physics beyond the SM.

Though the inclusive decay $B \to X_s\ell^+\ell^-$ is better understood theoretically using the operator product expansion, and the first direct experimental measurements of the dilepton invariant mass spectrum and m_X-distribution are already at hand [1, 2], being an inclusive process, it is extremely difficult to be measured in a hadron machine, such as the LHC, which is the only collider, except for a Super-B factory, that could provide enough luminosity for the precise study of the decay distributions of such a rare process. In contrast, for the exclusive decay $B \to K^*\ell^+\ell^-$, the difficulty lies in the imprecise knowledge of the underlying hadron dynamics. Experimentally, the BaBar [3] and Belle [4] Collaborations have observed this rare decay with the branching ratios

$$\mathrm{Br}(B \to K^*\ell^+\ell^-) = \begin{cases} (7.8^{+1.9}_{-1.7} \pm 1.2) \times 10^{-7} & (\mathrm{BaBar})\,, \\ (16.5^{+2.3}_{-2.2} \pm 0.9 \pm 0.4) \times 10^{-7} & (\mathrm{Belle})\,. \end{cases} \quad (1)$$

We note that the Belle measurements are approximately a factor 2 higher than the corresponding BaBar measurements. In addition, Belle has published the measurements [4, 5] of the so-called forward–backward asymmetry (FBA) [6]. In particular, the best-fit results by Belle for the Wilson coefficient ratios for a negative value of A_7,

$$\frac{A_9}{A_7} = -15.3^{+3.4}_{-4.8} \pm 1.1\,, \qquad \frac{A_{10}}{A_7} = 10.3^{+5.2}_{-3.5} \pm 1.8\,, \quad (2)$$

are consistent with the SM values $A_9/A_7 \simeq -13.7$ and $A_{10}/A_7 \simeq +14.9$, evaluated in the NLO approximation (see Table 1). With more data accumulated at the current B factories, and especially the huge data that will be produced at the LHC, it is foreseeable that the dilepton invariant mass spectrum and the FBA in this channel will be measured precisely in several years from now, allowing a few % measurements of the Wilson coefficient ratios and the sign of A_7.

[a] e-mail: ahmed.ali@desy.de
[b] e-mail: gustav.kramer@desy.de
[c] e-mail: guohuai.zhu@desy.de; Alexander-von-Humboldt Fellow

Table 1. The leading-logarithmic (LL) and next-to-leading-logarithmic (NLL) Wilson coefficients evaluated at the scale $m_{\rm b} = 4.8\,{\rm GeV}$. For $C_{9,10}$, they are also given in the NNLL order

	LL	NLL		LL	NLL	NNLL
$\bar{C}_1$	−0.2501	−0.1459	$\bar{C}_6$	−0.0316	−0.0388	
$\bar{C}_2$	1.1082	1.0561	$C_7^{\rm eff}$	−0.3145	−0.3054	
$\bar{C}_3$	0.0112	0.0116	$C_8^{\rm eff}$	−0.1491	−0.1678	
$\bar{C}_4$	−0.0257	−0.0337	C_9	1.9919	4.1777	4.2120
$\bar{C}_5$	0.0075	0.0097	C_{10}	0	−4.5415	−4.1958

Theoretically, the exclusive decay $B \to K^* \ell^+ \ell^-$ has been studied in a number of papers; see for example [7–12]. From the viewpoint of hadron dynamics, the application of the QCD factorization approach [13] to this channel [14] deserves special mention, as we shall be comparing our phenomenological analysis with the results obtained in this paper. The emergence of an effective theory, called soft-collinear effective theory (SCET) [15–19], provides a systematic and rigorous way to deal with the perturbative strong interaction effects in B decays in the heavy-quark expansion. A lot of theoretical work has been done in SCET related to the so-called heavy-to-light transitions in B decays; in particular, a demonstration of the soft-collinear factorization [20–23], a complete catalogue of the various 2-body and 3-body current operators [19, 22, 24], and the extension of SCET to two effective theories $\mathrm{SCET_I}$ and $\mathrm{SCET_{II}}$, with the two-step matching QCD $\to$ $\mathrm{SCET_I}$ $\to$ $\mathrm{SCET_{II}}$ [25]. Among various phenomenological applications reported in the literature, SCET has been used to prove the factorization of radiative $B \to V\gamma$ decays at leading power in $1/m_b$ and to all orders in $\alpha_{\rm s}$ [26, 27]. Likewise, SCET, in combination with the heavy-hadron chiral perturbation theory, has also been used to study the forward–backward asymmetry in the non-resonant decay $B \to K\pi\ell^+\ell^-$ in a certain kinematic region [28]. In this paper, our aim is to use SCET in the decay $B \to K^*\ell^+\ell^-$. Due to the similarity between $B \to K^*\gamma$ and $B \to K^*\ell^+\ell^-$ decays, our approach is quite similar to the earlier SCET-based studies [26, 27]; in particular to the one in [26]. Moreover, an analysis of the exclusive radiative and semileptonic decays $B \to K^*\gamma$ and $B \to K^*\ell^+\ell^-$ in SCET can be combined with data to reduce the uncertainties in the input parameters. In particular, as we show here, the location of the forward–backward asymmetry in $B \to K^*\ell^+\ell^-$ can be predicted more precisely than is the case in the existing literature.

It is well known that, when q^2, the momentum squared of the lepton pair, is comparable to $M_{J/\psi}^2$, the resonant charmonium contributions become very important, for which there is no model-independent treatment yet. Likewise, for higher q^2-values, higher ψ-resonances $(\psi', \psi'', \dots)$ have to be included. Thus, in the following we will restrict ourselves to the region $1\,{\rm GeV}^2 < q^2 < 7\,{\rm GeV}^2$, which is dominated by the short-distance contribution. Note that the lower cut-off $1\,{\rm GeV}^2$ is taken here because, as we shall see later, when q^2 is very small, say $q^2 \sim \mathcal{O}(\Lambda_{\rm QCD}^2)$, the factorization of the annihilation topology breaks down. In this kinematic region, a factorization formula for the decay amplitude of $B \to K^*\ell^+\ell^-$, which holds to $O(\alpha_{\rm s})$ at the leading power in $1/m_b$, has been derived in [14] using the QCD factorization approach. We shall derive the factorization of the decay amplitude of $B \to K^*\ell^+\ell^-$ in SCET, which *formally* coincides with the formula obtained by Beneke et al. [14] but is valid to all orders of $\alpha_{\rm s}$:

$$\langle K_a^* \ell^+ \ell^- | H_{\rm eff} | B \rangle = T_a^{\rm I}(q^2) \zeta_a(q^2) + \sum_{\pm} \int_0^\infty \frac{{\rm d}\omega}{\omega} \phi_\pm^B(\omega) \int_0^1 {\rm d}u \phi_{K^*}^a(u) T_{a,\pm}^{\rm II}(\omega, u, q^2)\,, \quad (3)$$

where $a = \|, \perp$ denotes the polarization of the K^* meson. The functions $T^{\rm I}$ and $T^{\rm II}$ are perturbatively calculable. $\zeta_a(q^2)$ are the soft form factors defined in SCET, while $\phi_\pm^B$ and $\phi_{K^*}^a$ are the light-cone distribution amplitudes (LCDAs) for the B and K^* mesons, respectively. Compared to the earlier results of [14], obtained in the QCD factorization approach, the main phenomenological improvement is that for the hard scattering function $T^{\rm II}$ the perturbative logarithms are summed from the hard scale $\mu_b \sim \mathcal{O}(m_b)$ down to the intermediate scale $\mu_\ell \equiv \sqrt{\mu_b \Lambda_h}$, where Λ_h represents a typical hadronic scale. Note also that the definitions of the soft form factors $\zeta_a(q^2)$ for our SCET currents, defined below in Sect. 2, are different from those of [14], a point to which we will return later in Sect. 3. Hence, the explicit expressions for $T^{\rm I}$ derived here and in [14] are also different.

This paper is organized as follows. In Sect. 2, we briefly review the basic ideas and notation of SCET. We then list the relevant effective operators in SCET and do the explicit matching calculations from QCD to $\mathrm{SCET_I}$ (Sect. 2.1) and from $\mathrm{SCET_I}$ to $\mathrm{SCET_{II}}$ (Sect. 2.2). The matrix elements of the effective SCET operators are given in Sect. 2.3. At the end of this section, the logarithmic resummation in $\mathrm{SCET_I}$ is discussed. In Sect. 3, we consider some phenomenological aspects of the $B \to K^*\ell^+\ell^-$ decay. We first specify the input parameters, especially the soft form factors $\zeta_{\perp,\|}(q^2)$ (Sect. 3.1), which are the cause of the largest theoretical uncertainty. We use the q^2-dependence of the related QCD form factors in the LC-QCD sum rule approach, but we fix the normalization of these soft form factors using constraints from data on the exclusive decays $B \to K^*\gamma$. In Sect. 3.2, we work out numerically the evolution of the B-type $\mathrm{SCET_I}$ matching coefficients, defined earlier in Sect. 2. We then give the dilepton invari-

ant mass spectrum and the forward–backward asymmetry in the decay $B \to K^* \ell^+ \ell^-$ and compare the integrated branching ratios with the measurements from BaBar and Belle (Sect. 3.3). We end with a summary of our results in Sect. 4 and suggestions for future measurements to reduce the model dependence due to the form factors and other input parameters.

2 SCET analysis of $B \to K^* \ell^+ \ell^-$

For the $b \to s$ transitions, the weak effective Hamiltonian can be written as

$$H_{\rm eff} = -\frac{G_{\rm F}}{\sqrt{2}} V_{ts}^* V_{tb} \sum_{i=1}^{10} C_i(\mu) Q_i(\mu)\,, \tag{4}$$

where we have neglected the contribution proportional to $V_{us}^* V_{ub}$ in the penguin (loop) amplitudes, which is doubly Cabibbo-suppressed, and we have used the unitarity of the CKM matrix to factorize the overall CKM-matrix element dependence. We use the operator basis as introduced in [14, 30]:

$$\begin{aligned}
Q_1 &= (\bar s\, T^A\, c)_{V-A} (\bar c\, T^A\, b)_{V-A}\,,\\
Q_2 &= (\bar s c)_{V-A} (\bar c b)_{V-A}\,,\\
Q_3 &= 2\,(\bar s b)_{V-A} \sum_q (\bar q \gamma^\mu q)\,,\\
Q_4 &= 2\,(\bar s\, T^A\, b)_{V-A} \sum_q (\bar q \gamma^\mu T^A\, q)\,,\\
Q_5 &= 2\,\bar s \gamma_\mu \gamma_\nu \gamma_\rho (1-\gamma_5) b \sum_q (\bar q \gamma^\mu \gamma^\nu \gamma^\rho q)\,,\\
Q_6 &= 2\,\bar s \gamma_\mu \gamma_\nu \gamma_\rho (1-\gamma_5) T^A\, b \sum_q (\bar q \gamma^\mu \gamma^\nu \gamma^\rho T^A\, q)\,,\\
Q_7 &= -\frac{g_{\rm em} \overline{m}_b}{8\pi^2} \bar s \sigma^{\mu\nu} (1+\gamma_5) b F_{\mu\nu}\,,\\
Q_8 &= -\frac{g_s \overline{m}_b}{8\pi^2} \bar s \sigma^{\mu\nu} (1+\gamma_5) T^A\, b\, G^A_{\mu\nu}\,,\\
Q_9 &= \frac{\alpha_{\rm em}}{2\pi} (\bar s b)_{V-A} (\bar \ell \gamma^\mu \ell)\,,\\
Q_{10} &= \frac{\alpha_{\rm em}}{2\pi} (\bar s b)_{V-A} (\bar \ell \gamma^\mu \gamma_5 \ell)\,,
\end{aligned} \tag{5}$$

where T^A is the $SU(3)$ color matrix, $\alpha_{\rm em} = g_{\rm em}^2/4\pi$ is the fine-structure constant, and $\overline{m}_b(\mu)$ is the current mass of the b-quark in the $\overline{\rm MS}$ scheme at the scale μ.

Restricting ourselves to the kinematic region $1\,{\rm GeV}^2 < q^2 < 7\,{\rm GeV}^2$, the light K^* meson moves fast, with a large momentum of the order of $m_B/2$, which thus can be viewed approximately as a collinear particle. For convenience, let us assume that the K^* meson is moving in the direction of the light-like reference vector n; then its momentum can be decomposed as $p^\mu = \bar n \cdot p\, n^\mu/2 + p_\perp^\mu + n \cdot p\, \bar n^\mu/2$, where $\bar n^\mu$ is another light-like reference vector satisfying $n \cdot \bar n = 2$. In this light-cone frame, the collinear momentum of K^* is expressed as

$$p = (n\cdot p, \bar n \cdot p, p_\perp) \sim (\lambda^2, 1, \lambda) m_b\,, \tag{6}$$

with $\lambda \sim \Lambda/m_b \ll 1$. In addition to this collinear mode, the soft- and hard-collinear modes, with momenta scaling as $(\lambda,\lambda,\lambda)m_b$ and $(\lambda, 1, \sqrt{\lambda})m_b$, respectively, are also necessary to correctly reproduce the infrared behavior of full QCD.

SCET introduces fields for every momentum mode, and we will encounter the following quark and gluon fields:

$$\begin{aligned}
&\xi_{\rm c} \sim \lambda\,, \quad A_{\rm c}^\mu \sim (\lambda^2, 1, \lambda)\,, \quad \xi_{\rm hc},\, \xi_{\overline{\rm hc}} \sim \lambda^{1/2}\,,\\
&A_{\rm hc}^\mu \sim (\lambda, 1, \lambda^{1/2})\,, \quad q_{\rm s} \sim \lambda^{3/2}\,, \quad A_{\rm s}^\mu \sim (\lambda,\lambda,\lambda)\,,\\
&h \sim \lambda^{3/2}\,.
\end{aligned} \tag{7}$$

In the above, the symbol A^μ stands for the gluon field, h represents a heavy-quark field, the symbols ξ and q stand for the light-quark fields, and the subscripts ${\rm c, s, hc}$ stand for collinear, soft- and hard-collinear modes, respectively. Note that the momentum q of the lepton pair is taken as a hard-collinear momentum, since in this paper we only consider the range $1\,{\rm GeV}^2 < q^2 < 7\,{\rm GeV}^2$. That is why an extra hard-collinear field $\xi_{\overline{\rm hc}}$ in the $\bar n$-direction is required later. As explained in detail in [26], to construct the gauge invariant operators in SCET, it is more convenient to introduce the building blocks, given below, which are obtained by multiplying the fields by the Wilson lines which run along the light-ray to infinity:

$$\mathcal{X}_{\rm c}\,,\ \mathcal{A}_{\rm c}^\mu\,,\ \mathcal{X}_{\rm hc}\,,\ \mathcal{X}_{\overline{\rm hc}}\,,\ \mathcal{A}_{\rm hc}^\mu\,,\ \mathcal{Q}_{\rm s}\,,\ \mathcal{A}_{\rm s}^\mu\,,\ \mathcal{H}_{\rm s}\,,\ \mathcal{Q}_{\bar{\rm s}}\,,\ \mathcal{H}_{\bar{\rm s}}\,. \tag{8}$$

For example, the field $\mathcal{X}_{\rm hc}$ is defined as

$$\begin{aligned}
&\mathcal{X}_{\rm hc}(x) = W_{\rm hc}^\dagger(x) \xi_{\rm hc}(x), \quad \text{with}\\
&W_{\rm hc}(x) = P \exp\left({\rm i} g \int_{-\infty}^0 {\rm d}s \bar n \cdot A_{\rm hc}(x + s\bar n) \right),
\end{aligned} \tag{9}$$

where $W_{\rm hc}(x)$ is the hard-collinear Wilson line. The notations $\mathcal{Q}_{\bar{\rm s}}$ and $\mathcal{H}_{\bar{\rm s}}$ are used when the associated soft Wilson lines are in the $\bar n$-direction. For the definitions of the other fields and more technical details about SCET, we refer the reader to [26] and references therein.

Since SCET contains two kinds of collinear fields, i.e. hard-collinear and collinear fields, normally an intermediate effective theory, called ${\rm SCET_I}$, is introduced which contains only soft- and hard-collinear fields, while the final effective theory, called ${\rm SCET_{II}}$, contains only soft and collinear fields. We will then do a two-step matching from ${\rm QCD} \to {\rm SCET_I} \to {\rm SCET_{II}}$.

2.1 QCD to ${\rm SCET_I}$ matching

In ${\rm SCET_I}$, the K^* meson is taken as a hard-collinear particle and the relevant building blocks are $\mathcal{X}_{\rm hc}$, $\mathcal{X}_{\overline{\rm hc}}$, $\mathcal{A}_{\rm hc}^\mu$ and h. The velocity of the B meson is defined as $v = P_B/m_B$. The matching from QCD to ${\rm SCET_I}$ at leading power may

be expressed as

$$H_{\rm eff} \to -\frac{G_{\rm F}}{\sqrt{2}} V_{ts}^* V_{tb} \Bigg(\sum_{i=1}^{4} \int {\rm d}s\, \widetilde{C}_i^A\,(s) J_i^A\,(s) + \sum_{j=1}^{4} \int {\rm d}s \int {\rm d}r\, \widetilde{C}_j^B(s,r) J_j^B(s,r) + \int {\rm d}s \int {\rm d}r \int {\rm d}t\, \widetilde{C}^C(s,r,t) J^C(s,r,t) \Bigg) , \tag{10}$$

where $\widetilde{C}_i^{(A,B)}$ and $\widetilde{C}^C$ are Wilson coefficients in position space. The relevant $\mathrm{SCET_I}$ operators for the $B \to K^* \ell^+ \ell^-$ decay are constructed by using the building blocks mentioned above [26]:

$$\begin{aligned}
J_1^A &= \bar{\mathcal{X}}_{\rm hc}(s\bar{n})(1+\gamma_5)\gamma_\perp^\mu h(0)\; \bar{\ell}\gamma_\mu \ell\,, \\
J_2^A &= \bar{\mathcal{X}}_{\rm hc}(s\bar{n})(1+\gamma_5)\frac{n^\mu}{n\cdot v} h(0)\; \bar{\ell}\gamma_\mu \ell\,, \\
J_3^A &= \bar{\mathcal{X}}_{\rm hc}(s\bar{n})(1+\gamma_5)\gamma_\perp^\mu h(0)\; \bar{\ell}\gamma_\mu\gamma_5 \ell\,, \\
J_4^A &= \bar{\mathcal{X}}_{\rm hc}(s\bar{n})(1+\gamma_5)\frac{n^\mu}{n\cdot v} h(0)\; \bar{\ell}\gamma_\mu\gamma_5 \ell\,, \\
J_1^B &= \bar{\mathcal{X}}_{\rm hc}(s\bar{n})(1+\gamma_5)\gamma_\perp^\mu \mathcal{A}_{{\rm hc}\perp}(r\bar{n}) h(0)\; \bar{\ell}\gamma_\mu \ell\,, \\
J_2^B &= \bar{\mathcal{X}}_{\rm hc}(s\bar{n})(1+\gamma_5)\mathcal{A}_{{\rm hc}\perp}(r\bar{n})\frac{n^\mu}{n\cdot v} h(0)\; \bar{\ell}\gamma_\mu \ell\,, \\
J_3^B &= \bar{\mathcal{X}}_{\rm hc}(s\bar{n})(1+\gamma_5)\gamma_\perp^\mu \mathcal{A}_{{\rm hc}\perp}(r\bar{n}) h(0)\; \bar{\ell}\gamma_\mu\gamma_5 \ell\,, \\
J_4^B &= \bar{\mathcal{X}}_{\rm hc}(s\bar{n})(1+\gamma_5)\mathcal{A}_{{\rm hc}\perp}(r\bar{n})\frac{n^\mu}{n\cdot v} h(0)\; \bar{\ell}\gamma_\mu\gamma_5 \ell\,, \\
J^C &= \bar{\mathcal{X}}_{\rm hc}(s\bar{n})(1+\gamma_5)\frac{\bar{n}\!\!\!/}{2}\mathcal{X}_{\rm hc}(r\bar{n})\; \bar{\mathcal{X}}_{\overline{\rm hc}}(an)(1+\gamma_5)\frac{n\!\!\!/}{2} h(0)\,,
\end{aligned} \tag{11}$$

where the operators J_i^A and J_j^B represent the cases that the lepton pair is emitted from the $b \to s$ transition currents, while J^C represents the diagrams in which the lepton pair is emitted from the spectator quark of the B meson. Except for the lepton pair, the operators $J_i^{A,B}$ have the same Dirac structures as those of the heavy-to-light transition currents in SCET, which were first derived in [16] for J_i^A and in [24, 25] for J_j^B (see also [23, 31]). In this paper we take the operator basis of [26, 31] which makes J_j^B multiplicatively renormalized, but we have neglected the operators which contain the Dirac structure $\mathcal{A}_{{\rm hc}\perp}\gamma_\perp^\mu$ and which do not contribute to the exclusive B meson decays. It is also clear that the structure $\bar{\ell}\gamma_\mu\gamma_5\ell$ arises solely from Q_{10} of the weak effective Hamiltonian.

Since in practice the matching calculations are done in the momentum space, it is more convenient to define the Wilson coefficients in the momentum space by the following Fourier-transformations:

$$\begin{aligned}
C_i^A(E) &= \int {\rm d}s\; {\rm e}^{{\rm i}s\bar{n}\cdot P} \widetilde{C}_i^A(s)\,, \\
C_j^B(E,u) &= \int {\rm d}s \int {\rm d}r\; {\rm e}^{{\rm i}(us+\bar{u}r)\bar{n}\cdot P} \widetilde{C}_j^B(s,r)\,, \\
C^C(E,u) &= \int {\rm d}s \int {\rm d}r \int {\rm d}a\; {\rm e}^{{\rm i}(us+\bar{u}r)\bar{n}\cdot P} {\rm e}^{{\rm i}an\cdot q} \widetilde{C}^C(s,r,a)\,,
\end{aligned} \tag{12}$$

with $E \equiv n\cdot v\bar{n}\cdot P/2$ and $\bar{u} = 1-u$. To get the order $\alpha_{\rm s}$ corrections to the decay amplitude, we need to calculate the Wilson coefficients C_i^A to one-loop level and C_j^B and C^C to tree level. In the following we will use $\Delta_j C_i^{(A,B,C)}$ to denote the matching results from the weak effective operators Q_j to the SCET currents $J_i^{A,B,C}$. With this, the matching coefficients from QCD $\to \mathrm{SCET_I}$ can be written as

$$C_i^{(A,B,C)} = \sum_{j=1}^{10} \Delta_j C_i^{(A,B,C)}(\mu_{\rm QCD}, \mu)\,, \tag{13}$$

where $\mu_{\rm QCD}$ is the matching scale and μ is the renormalization scale in $\mathrm{SCET_I}$.

Each operator of the weak effective Hamiltonian, namely Q_{1-10}, will contribute to C_i^A at order $\alpha_{\rm s}$ level, as shown in Fig. 1. But due to the small Wilson coefficients C_{3-6}, it is numerically reasonable to neglect the contributions from Q_{3-6}. For the operators $Q_{1,2}$ and Q_8, the results

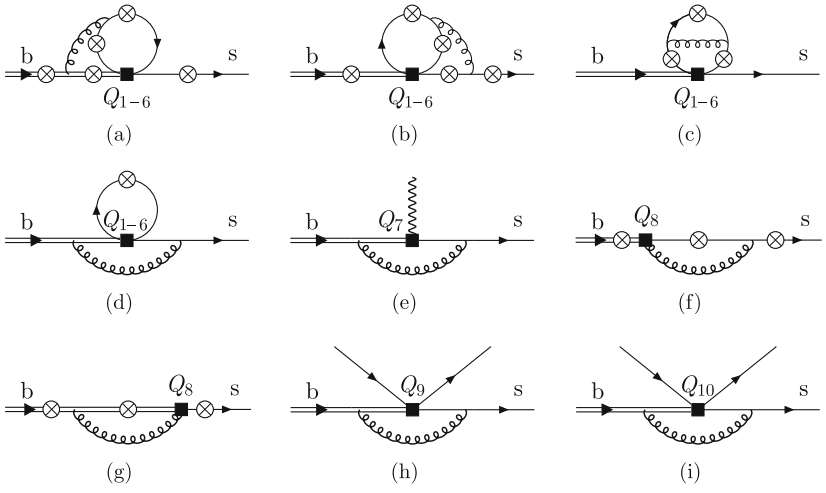

Fig. 1. $\mathcal{O}(\alpha_{\rm s})$ contributions to the matching of Q_i to A-type SCET currents. The *crossed circles* denote the possible locations from where the virtual photon is emitted and then splits into a lepton pair

can be easily derived from (11) and (25) of [32]:

$$\begin{aligned}
&\Delta_{1,2} C_1^A(\mu_{\rm QCD}) = -\frac{\alpha_{\rm em}}{2\pi}\frac{\alpha_{\rm s}(\mu_{\rm QCD})}{4\pi} \\
&\times \left[\frac{1}{\hat{s}}\left(2F_2^{(7)} + \hat{s}F_2^{(9)}\right)\bar{C}_2 + 2\left(F_1^{(9)} + F_2^{(9)}/6\right)\bar{C}_1\right], \\
&\Delta_{1,2} C_2^A(\mu_{\rm QCD}) = -\frac{\alpha_{\rm em}}{2\pi}\frac{\alpha_{\rm s}(\mu_{\rm QCD})}{4\pi} \\
&\times \left[\left(2F_2^{(7)} + F_2^{(9)}\right)\bar{C}_2 + 2\left(F_1^{(9)} + F_2^{(9)}/6\right)\bar{C}_1\right], \\
&\Delta_8 C_1^A(\mu_{\rm QCD}) = \\
&-\frac{\alpha_{\rm em}}{2\pi}\frac{\alpha_{\rm s}(\mu_{\rm QCD})}{4\pi}\frac{\overline{m}_b(\mu_{\rm QCD})}{m_b}\left[\frac{2}{\hat{s}}F_8^{(7)} + F_8^{(9)}\right]C_8^{\rm eff}, \\
&\Delta_8 C_2^A(\mu_{\rm QCD}) = \\
&-\frac{\alpha_{\rm em}}{2\pi}\frac{\alpha_{\rm s}(\mu_{\rm QCD})}{4\pi}\frac{\overline{m}_b(\mu_{\rm QCD})}{m_b}\left[2F_8^{(7)} + F_8^{(9)}\right]C_8^{\rm eff}, \quad (14)
\end{aligned}$$

where $\hat{s} \equiv q^2/m_b^2$, and m_b is the pole mass of the b-quark. The current mass $\overline{m}_b$ is related to the pole mass at next-to-leading order by

$$\overline{m}_b(\mu) = m_b\left[1 + \frac{\alpha_{\rm s} C_F}{4\pi}\left(3\ln\frac{m_b^2}{\mu^2} - 4\right)\right], \quad (15)$$

where $C_F = 4/3$. The functions $F_{1,2,8}^{(7,9)}$ are given in a mixed analytic and numerical form in [32]. Following the convention of [14], we also use the "barred" coefficients $\bar{C}_i$ $(i = 1, \ldots, 6)$ here which are the linear combinations of the Wilson coefficients C_i of the weak effective Hamiltonian in (4). The effective Wilson coefficient $C_8^{\rm eff}$ is defined as $C_8^{\rm eff} = C_8 + C_3 - C_4/6 + 20C_5 - 10C_6$.

For the operators Q_7, Q_9 and Q_{10}, the matchings to the A-type currents give

$$\begin{aligned}
\Delta_7 C_1^A &= \frac{\alpha_{\rm em}}{2\pi}\frac{\overline{m}_b(\mu_{\rm QCD})}{m_b}\frac{2}{\hat{s}}\widetilde{C}_9 C_7^{\rm eff}, \\
\Delta_7 C_2^A &= \frac{\alpha_{\rm em}}{2\pi}\frac{\overline{m}_b(\mu_{\rm QCD})}{m_b} 2\widetilde{C}_{10} C_7^{\rm eff}, \\
\Delta_9 C_1^A &= \frac{\alpha_{\rm em}}{2\pi}\widetilde{C}_3 C_9^{\rm eff}, \\
\Delta_9 C_2^A &= \frac{\alpha_{\rm em}}{2\pi}\left(\widetilde{C}_4 + \frac{1-\hat{s}}{2}\widetilde{C}_5\right)C_9^{\rm eff}, \\
\Delta_{10} C_3^A &= \frac{\alpha_{\rm em}}{2\pi}\widetilde{C}_3 C_{10}, \\
\Delta_{10} C_4^A &= \frac{\alpha_{\rm em}}{2\pi}\left(\widetilde{C}_4 + \frac{1-\hat{s}}{2}\widetilde{C}_5\right)C_{10}. \quad (16)
\end{aligned}$$

To avoid confusion with the Wilson coefficients in (4), we use the notation $\widetilde{C}_i$ for the matching coefficients, instead of C_i as used originally in [16]. The explicit expressions of $\widetilde{C}_i$ up to one-loop order can be read from [16, 23]. Note that although the operator basis of the tensor current in [23] looks slightly different from that of [16]; they are actually the same, and it is easy to find the relations $\widetilde{C}_9 = C_T^{(A0)2}$ and $\widetilde{C}_{10} = C_T^{(A0)1}$. The effective Wilson coefficients are defined as $C_7^{\rm eff} = C_7 - C_3/3 - 4C_4/9 - 20C_5/3 - 80C_6/9$ and $C_9^{\rm eff}(q^2) = C_9 + Y(q^2)$, where the function $Y(q^2)$ represents the contributions of the fermion loops and the explicit formula can be found in [14].

To get the decay amplitude of $B \to K^* \ell^+ \ell^-$ in order $\alpha_{\rm s}$, the tree-level matching of the effective weak Hamiltonian (4) onto the B-type SCET currents (11) is already enough, as illustrated in Fig. 2. If we let the notation $\Delta_{16} C_i^B$ stand for the matchings of Q_{1-6} onto the B-type SCET currents J_i^B, namely $\Delta_{16} C_i^B \equiv \sum_{j=1}^6 \Delta_j C_i^B$, we get from Fig. 2a that

$$\begin{aligned}
\Delta_{16} C_1^B &= -\frac{\alpha_{\rm em}}{2\pi}\frac{1}{m_b \hat{s}}\left(\frac{2}{3}F_{16}^{\perp}\left(u, \hat{s}, m_c^2/m_b^2\right)\left(\bar{C}_2 + \bar{C}_4 - \bar{C}_6\right)\right. \\
&\quad - \frac{1}{3}F_{16}^{\perp}(u, \hat{s}, 0)\bar{C}_3 \\
&\quad \left. - \frac{1}{3}F_{16}^{\perp}(u, \hat{s}, 1)\left(\bar{C}_3 + \bar{C}_4 - \bar{C}_6 - 4\bar{C}_5\right)\right), \\
\Delta_{16} C_2^B &= \frac{\alpha_{\rm em}}{2\pi}\frac{2}{m_b}\left(\frac{2}{3}F_{16}^{\parallel}\left(u, \hat{s}, m_c^2/m_b^2\right)\left(\bar{C}_2 + \bar{C}_4 - \bar{C}_6\right)\right. \\
&\quad - \frac{1}{3}F_{16}^{\parallel}(u, \hat{s}, 0)\bar{C}_3 \\
&\quad \left. - \frac{1}{3}F_{16}^{\parallel}(u, \hat{s}, 1)\left(\bar{C}_3 + \bar{C}_4 - \bar{C}_6\right)\right), \quad (17)
\end{aligned}$$

where u is the momentum fraction carried by the strange quark in the K^* meson. The functions $F_{16}^{\perp,\parallel}$ are defined as

$$\begin{aligned}
&F_{16}^{\perp}(u, \hat{s}, \lambda) \\
&= 1 + \frac{2}{(1-\hat{s})(1-u)}\left(\hat{s}\left(\frac{\sqrt{-\hat{s}+4\lambda}}{\sqrt{\hat{s}}}\arctan\frac{\sqrt{\hat{s}}}{\sqrt{-\hat{s}+4\lambda}}\right.\right. \\
&\quad \left.\left. - \frac{\sqrt{-1+u-\hat{s}u+4\lambda}}{\sqrt{1-(1-\hat{s})u}}\arctan\frac{\sqrt{1-(1-\hat{s})u}}{\sqrt{-1+u-\hat{s}u+4\lambda}}\right)\right.
\end{aligned}$$

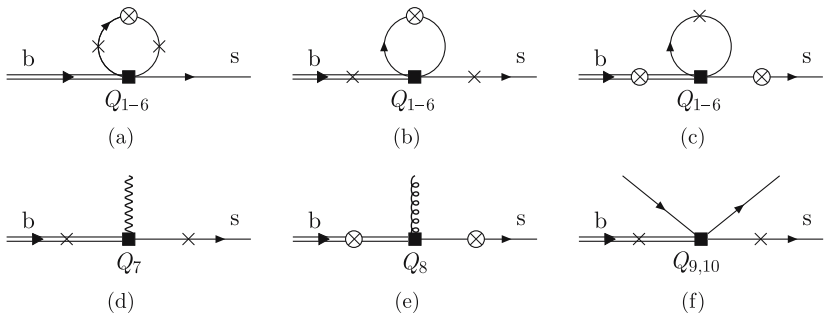

Fig. 2. Tree-level matching of Q_i onto B-type SCET currents. The *crossed circles* denote the possible locations from where the virtual photon is emitted, while the *crosses* mark the possible places where a gluon line may be attached

$$
\begin{aligned}
&+\lambda\,\mathrm{Li}_2\left(\frac{2\sqrt{\hat{s}}}{\sqrt{\hat{s}}-\sqrt{\hat{s}-4\lambda}}\right)+\lambda\,\mathrm{Li}_2\left(\frac{2\sqrt{\hat{s}}}{\sqrt{\hat{s}}+\sqrt{\hat{s}-4\lambda}}\right)\\
&-\lambda\,\mathrm{Li}_2\left(\frac{2\sqrt{1-(1-\hat{s})u}}{\sqrt{1-(1-\hat{s})u}+\sqrt{1-(1-\hat{s})u-4\lambda}}\right)\\
&-\lambda\,\mathrm{Li}_2\left(\frac{2\sqrt{1-(1-\hat{s})u}}{\sqrt{1-(1-\hat{s})u}-\sqrt{1-(1-\hat{s})u-4\lambda}}\right)\Bigg)\,,
\end{aligned}
\tag{18}
$$

$$
\begin{aligned}
&F_{16}^{\parallel}(u,\hat{s},\lambda)\\
&=2\hat{s}+\frac{4\hat{s}}{(1-\hat{s})(1-u)}\Bigg((1-u+u\hat{s})\\
&\times\left(\frac{\sqrt{-\hat{s}+4\lambda}}{\sqrt{\hat{s}}}\arctan\frac{\sqrt{\hat{s}}}{\sqrt{-\hat{s}+4\lambda}}\right.\\
&\left.-\frac{\sqrt{-1+u-\hat{s}u+4\lambda}}{\sqrt{1-(1-\hat{s})u}}\arctan\frac{\sqrt{1-(1-\hat{s})u}}{\sqrt{-1+u-\hat{s}u+4\lambda}}\right)\\
&+\lambda\,\mathrm{Li}_2\left(\frac{2\sqrt{\hat{s}}}{\sqrt{\hat{s}}-\sqrt{\hat{s}-4\lambda}}\right)+\lambda\,\mathrm{Li}_2\left(\frac{2\sqrt{\hat{s}}}{\sqrt{\hat{s}}+\sqrt{\hat{s}-4\lambda}}\right)\\
&-\lambda\,\mathrm{Li}_2\left(\frac{2\sqrt{1-(1-\hat{s})u}}{\sqrt{1-(1-\hat{s})u}+\sqrt{1-(1-\hat{s})u-4\lambda}}\right)\\
&-\lambda\,\mathrm{Li}_2\left(\frac{2\sqrt{1-(1-\hat{s})u}}{\sqrt{1-(1-\hat{s})u}-\sqrt{1-(1-\hat{s})u-4\lambda}}\right)\Bigg)\,.
\end{aligned}
\tag{19}
$$

As a check, it is not difficult to find the following relations:

$$
\begin{aligned}
F_{16}^{\perp}(u,\hat{s},\frac{m_q^2}{m_b^2})&=t_\perp(u,m_q)\frac{(1-u)E}{2M_B}\,,\\
F_{16}^{\parallel}(u,\hat{s},\frac{m_q^2}{m_b^2})&=t_\parallel(u,m_q)\frac{\hat{s}(1-u)E}{M_B}\,,
\end{aligned}
$$

where the functions $t_{\perp,\parallel}(u,m_q)$ are defined in (27) and (28) in the paper by Beneke et al. [14]. We also note that the functions $F_{16}^{\perp}(u,\hat{s},\lambda)$ and $F_{16}^{\parallel}(u,\hat{s},\lambda)$ are finite as $\bar{u}=1-u\to 0$, as opposed to the functions $t_{\perp,\parallel}(u,m_q)$, which are singular as $\bar{u}\to 0$.

Figure 2d and the operator Q_9 of Fig. 2f, combined with Fig. 2b, will contribute to the matching coefficients $\Delta_{7,9}C_{1,2}^B$, while the operator Q_{10} of Fig. 2f will contribute to $\Delta_{10}C_{3,4}^B$:

$$
\begin{aligned}
\Delta_7 C_1^B&=-\frac{\alpha_{\rm em}}{2\pi}\frac{\overline{m}_b}{m_b^2\hat{s}}2C_7^{\rm eff}\,,\\
\Delta_7 C_2^B&=\frac{\alpha_{\rm em}}{2\pi}\frac{\overline{m}_b}{m_b^2(1-\hat{s})}2C_7^{\rm eff}\,,\\
\Delta_9 C_1^B&=0\,,\quad \Delta_9 C_2^B=-\frac{\alpha_{\rm em}}{2\pi}\frac{1-2\hat{s}}{m_b(1-\hat{s})}C_9^{\rm eff}\,,\\
\Delta_{10} C_3^B&=0\,,\quad \Delta_{10} C_4^B=-\frac{\alpha_{\rm em}}{2\pi}\frac{1-2\hat{s}}{m_b(1-\hat{s})}C_{10}\,.
\end{aligned}
\tag{20}
$$

Finally, Fig. 2e and c contribute to the matching coefficients

$$
\Delta_8 C_1^B=-\frac{\alpha_{\rm em}}{2\pi}\frac{\overline{m}_b}{m_b^2}\frac{2(1-u)(1-\hat{s})}{3\hat{s}(u+\hat{s}-u\hat{s})}C_8^{\rm eff}\,,\quad \Delta_8 C_2^B=0\,.
\tag{21}
$$

We shall now consider the diagrams where the virtual (off-shell) photon is emitted from the spectator quark, as shown in Fig. 3. Due to the off-shellness of the quark propagator, it is easy to check that Fig. 3d–f are of order $1/m_b$ suppressed compared with Fig. 3a–c, where the photon is emitted from the spectator quark in the B meson. Therefore at leading power in $1/m_b$, only the first three diagrams in Fig. 3 are relevant for our analysis. As we shall see in the following, all of these three diagrams contribute to the Wilson coefficients of the C-type SCET current.

The annihilation diagram, shown in Fig. 3a, contributes to the matching coefficient C^C at order $\alpha_{\rm s}^0$, for which the calculation is trivial:

$$
\Delta_{16}^{(0)}C^C=\frac{2}{3}\left(-\frac{V_{us}^*V_{ub}}{V_{ts}^*V_{tb}}(\bar{C}_1+3\bar{C}_2)\delta_{qu}+(\bar{C}_3+3\bar{C}_4)\right)\,.
\tag{22}
$$

Here q is the flavor of the spectator quark in the B meson and the superscript (0) denotes the matching at order $\alpha_{\rm s}^0$. At order $\alpha_{\rm s}$, the diagrams shown in Fig. 3b–c also contribute to the matching onto the C-type SCET current

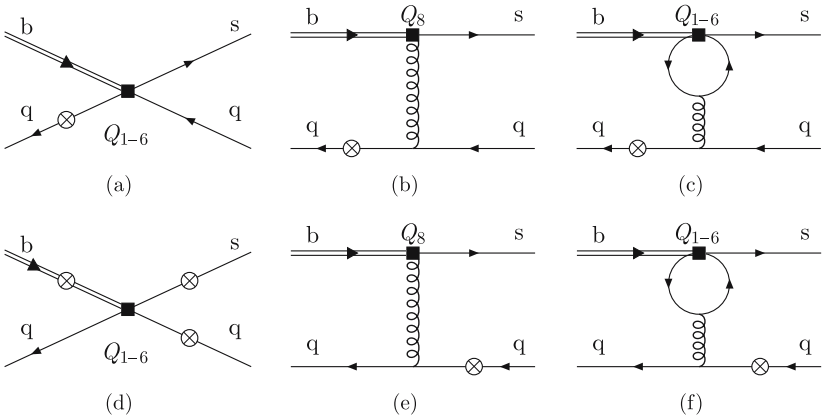

Fig. 3. The diagrams where the virtual photon, as denoted by the *crossed circle*, is emitted from the spectator quark

with the coefficients

$$\begin{aligned}
\Delta_8 C^C &= \frac{C_F}{N_c}\frac{\alpha_s}{4\pi}\frac{-4C_8^{\rm eff}}{1-u+u\hat{s}}\,,\\
\Delta_{16}^{(1)} C^C &= 2\frac{C_F}{N_c}\frac{\alpha_s}{4\pi}\Big\{ \left(\bar{C}_2+\bar{C}_4+\bar{C}_6\right) G\left(u,\hat{s},m_c^2/m_b^2\right)\\
&\quad + \left(\bar{C}_3+3\bar{C}_4+3\bar{C}_6\right) G\left(u,\hat{s},0\right)\\
&\quad + \left(\bar{C}_3+\bar{C}_4+\bar{C}_6\right) G\left(u,\hat{s},1\right)\\
&\quad + \frac{4}{9}\left(\bar{C}_3-\bar{C}_5-15\bar{C}_6\right)\Big\}\,,
\end{aligned} \tag{23}$$

where the function $G(u,\hat{s},\lambda)$ is defined as

$$\begin{aligned}
G(u,\hat{s},\lambda) &= \frac{2}{3}+\frac{2}{3}\ln\frac{m_b^2}{\mu^2}\\
&\quad + 4\int_0^1 {\rm d}x\, x(1-x)\ln[\lambda - x(1-x)(1-u+u\hat{s})]\,.
\end{aligned} \tag{24}$$

2.2 $\mathbf{SCET_I \to SCET_{II}}$ matching

As shown in [21, 25], which analyzed the form factors in the framework of SCET, one may simply define the matrix elements of the A-type $\mathrm{SCET_I}$ currents as non-perturbative input since the non-factorizable parts of the form factors are all contained in such matrix elements. Therefore the explicit matching of J_i^A to $\mathrm{SCET_{II}}$ operators is not necessary here.

For B-type $\mathrm{SCET_I}$ operators, they are matched onto the following $\mathrm{SCET_{II}}$ operators:

$$\begin{aligned}
O_1^B &= \bar{\mathcal{X}}_{\rm c}(s\bar{n})(1+\gamma_5)\gamma_\perp^\mu\frac{\bar{n}\!\!\!/}{2}\mathcal{X}_{\rm c}(0)\\
&\quad\times \bar{\mathcal{Q}}_{\rm s}(tn)(1-\gamma_5)\frac{n\!\!\!/}{2}\mathcal{H}_{\rm s}(0)\,\bar{\ell}\gamma_\mu\ell\,,\\
O_2^B &= \bar{\mathcal{X}}_{\rm c}(s\bar{n})(1+\gamma_5)\frac{n^\mu}{n\cdot v}\frac{\bar{n}\!\!\!/}{2}\mathcal{X}_{\rm c}(0)\\
&\quad\times \bar{\mathcal{Q}}_{\rm s}(tn)(1+\gamma_5)\frac{n\!\!\!/}{2}\mathcal{H}_{\rm s}(0)\,\bar{\ell}\gamma_\mu\ell\,,\\
O_3^B &= \bar{\mathcal{X}}_{\rm c}(s\bar{n})(1+\gamma_5)\gamma_\perp^\mu\frac{\bar{n}\!\!\!/}{2}\mathcal{X}_{\rm c}(0)\\
&\quad\times \bar{\mathcal{Q}}_{\rm s}(tn)(1-\gamma_5)\frac{n\!\!\!/}{2}\mathcal{H}_{\rm s}(0)\,\bar{\ell}\gamma_\mu\gamma_5\ell\,,\\
O_4^B &= \bar{\mathcal{X}}_{\rm c}(s\bar{n})(1+\gamma_5)\frac{n^\mu}{n\cdot v}\frac{\bar{n}\!\!\!/}{2}\mathcal{X}_{\rm c}(0)\\
&\quad\times \bar{\mathcal{Q}}_{\rm s}(tn)(1+\gamma_5)\frac{n\!\!\!/}{2}\mathcal{H}_{\rm s}(0)\,\bar{\ell}\gamma_\mu\gamma_5\ell\,,
\end{aligned} \tag{25}$$

where we only include the color-singlet operators that have non-zero matrix elements for the $B \to K^*\ell^+\ell^-$ decay. Again, it is in practice more convenient to do the matching calculations in the momentum space, and the Wilson coefficients $D_i^B(\omega,u)$ can be defined by Fourier transforming the corresponding ones, $\tilde{D}_i^B(s,t)$, introduced in position space, just like the case in $\mathrm{SCET_I}$,

$$D_i^B(\omega,u) = \int {\rm d}s \int {\rm d}t\, {\rm e}^{-{\rm i}\omega n\cdot vt}{\rm e}^{{\rm i}us\bar{n}\cdot P}\tilde{D}_i^B(s,t). \tag{26}$$

Following the notation of [26], the Wilson coefficients D_i^B can be expressed as

$$\begin{aligned}
&D_i^B(\omega,u,\hat{s},\mu)\\
&= \frac{1}{\omega}\int_0^1 {\rm d}v\; \mathcal{J}_i\left(u,v,\ln\frac{m_b\omega(1-\hat{s})}{\mu^2},\mu\right) C_i^B(v,\mu)\,,
\end{aligned} \tag{27}$$

where the jet functions $\mathcal{J}_i$ arise from the $\mathrm{SCET_I} \to \mathrm{SCET_{II}}$ matching, and it is clear that $\mathcal{J}_1 = \mathcal{J}_3 \equiv \mathcal{J}_\perp$ and $\mathcal{J}_2 = \mathcal{J}_4 \equiv \mathcal{J}_\parallel$. At tree level, using the Fierz transformation in the operator basis,

$$\begin{aligned}
&\bar{\mathcal{X}}_{\rm c} N\mathcal{H}_{\rm s}\;\bar{\mathcal{Q}}_{\rm s}M\mathcal{X}_{\rm c}\\
&= -\frac{1}{4}\bar{\mathcal{X}}_{\rm c}(1+\gamma_5)\frac{\bar{n}\!\!\!/}{2}\mathcal{X}_{\rm c}\;\bar{\mathcal{Q}}_{\rm s}M(1-\gamma_5)\times\frac{n\!\!\!/}{2}N\mathcal{H}_{\rm s}\\
&\quad -\frac{1}{4}\bar{\mathcal{X}}_{\rm c}(1-\gamma_5)\frac{\bar{n}\!\!\!/}{2}\mathcal{X}_{\rm c}\bar{\mathcal{Q}}_{\rm s}M(1+\gamma_5)\frac{n\!\!\!/}{2}N\mathcal{H}_{\rm s}\\
&\quad -\frac{1}{8}\bar{\mathcal{X}}_{\rm c}(1+\gamma_5)\frac{\bar{n}\!\!\!/}{2}\gamma_{\perp\alpha}\mathcal{X}_{\rm c}\;\bar{\mathcal{Q}}_{\rm s}M(1+\gamma_5)\gamma_\perp^\alpha\frac{n\!\!\!/}{2}N\mathcal{H}_{\rm s}\,,
\end{aligned} \tag{28}$$

one obtains

$$\mathcal{J}_\perp(u,v) = \mathcal{J}_\parallel(u,v) = -\frac{4\pi C_F\alpha_s}{N_c}\frac{1}{m_b(1-u)(1-\hat{s})}\delta(u-v). \tag{29}$$

Finally, the C-type $\mathrm{SCET_I}$ current is matched onto the $\mathrm{SCET_{II}}$ operator

$$\begin{aligned}
O^C &= \bar{\mathcal{X}}_{\rm c}(s\bar{n})(1+\gamma_5)\frac{\bar{n}\!\!\!/}{2}\mathcal{X}_{\rm c}(0)\;\bar{\mathcal{Q}}_{\bar{\rm s}}(t\bar{n})(1+\gamma_5)\\
&\quad\times\frac{n\!\!\!/}{2}\mathcal{H}_{\bar{\rm s}}(0)\;\frac{\bar{n}^\mu}{\bar{n}\cdot v}\bar{\ell}\gamma_\mu\ell\,.
\end{aligned} \tag{30}$$

We may similarly define

$$D^C(\omega,u) = \int {\rm d}s \int {\rm d}t\; {\rm e}^{-{\rm i}\omega\bar{n}\cdot vt}{\rm e}^{{\rm i}us\bar{n}\cdot P}\tilde{D}^C(s,t), \tag{31}$$

with

$$\begin{aligned}
D^C(\omega,u,\hat{s},\mu) &= \frac{-ee_q\hat{s}}{(\omega - q^2/m_b - {\rm i}\epsilon)}\mathcal{J}^C\left(\ln\frac{m_b\omega(1-\hat{s})}{\mu^2},\mu\right)\\
&\quad\times C^C(E,u,\mu)\,,
\end{aligned} \tag{32}$$

where e_q is the electric charge of the spectator quark in the B meson. Note that the prefactor in (32), $-ee_q\hat{s}/(\omega - q^2/m_b - {\rm i}\epsilon)$, has been factored out from the definition of $\mathcal{J}^C$. The denominator of this prefactor comes from the propagator of the hard-collinear spectator quark, as seen in Fig. 3. With this, at tree level the corresponding jet function is trivial, $\mathcal{J}^C = 1$. For later convenience, we will define $D^C \equiv \widehat{D}^C/(\omega - q^2/m_b - {\rm i}\epsilon)$.

2.3 Matrix elements of SCET operators

The last step before we can finally get the decay amplitude for the $B \to K^*\ell^+\ell^-$ decay is to take the matrix elements of the relevant SCET operators. Since the soft and collinear

parts do not factorize in the matrix elements of the operator $\mathcal{J}^A$ in $\mathrm{SCET_{II}}$ due to an end-point singularity, we will define the matrix elements of the $\mathcal{J}^A$ current in $\mathrm{SCET_I}$. Following [26], they may be defined as follows:

$$\big\langle M(p)|\bar{\mathcal{X}}_{\rm hc}\Gamma h|B(v)\big\rangle = -2E\zeta_M(E)\mathrm{tr}\left[\overline{\mathcal{M}}_M(n)\Gamma\mathcal{M}_B(v)\right], \tag{33}$$

where the projection operators are

$$\begin{aligned}\mathcal{M}_B(v) &= -\frac{1+\not v}{2}\gamma_5\,, \quad \overline{\mathcal{M}}_{K^*_\perp}(n) = \not\varepsilon^*_\perp\frac{\not{\bar n}\not n}{4}\,,\\ \overline{\mathcal{M}}_{K^*_\parallel}(n) &= -\frac{\not{\bar n}\not n}{4}\,,\end{aligned} \tag{34}$$

with $\varepsilon^\mu_\perp$ being the polarization vector of the $K^*_\perp$ meson. It is then straightforward to get the matrix elements of the $\mathrm{SCET_I}$ currents J^A_i as

$$\begin{aligned}\big\langle K^*\ell^+\ell^-|J^A_1|B\big\rangle &= -2E\zeta_\perp\big(g^{\mu\nu}_\perp - \mathrm{i}\epsilon^{\mu\nu}_\perp\big)\varepsilon^*_{\perp\nu}\bar\ell\gamma_\mu\ell\,,\\ \big\langle K^*\ell^+\ell^-|J^A_2|B\big\rangle &= -2E\zeta_\parallel\frac{n^\mu}{n\cdot v}\bar\ell\gamma_\mu\ell\,,\\ \big\langle K^*\ell^+\ell^-|J^A_3|B\big\rangle &= -2E\zeta_\perp\big(g^{\mu\nu}_\perp - \mathrm{i}\epsilon^{\mu\nu}_\perp\big)\varepsilon^*_{\perp\nu}\bar\ell\gamma_\mu\gamma_5\ell\,,\\ \big\langle K^*\ell^+\ell^-|J^A_4|B\big\rangle &= -2E\zeta_\parallel\frac{n^\mu}{n\cdot v}\bar\ell\gamma_\mu\gamma_5\ell\,,\end{aligned} \tag{35}$$

where $g^{\mu\nu}_\perp \equiv g^{\mu\nu} - (n^\mu\bar n^\nu + \bar n^\mu n^\nu)/2$ and $\epsilon^{\mu\nu}_\perp \equiv \epsilon^{\mu\nu\rho\sigma}v_\rho n_\sigma/(n\cdot v)$. Note that, in the above equations, we use the convention $\epsilon^{0123} = +1$, as adopted in the book by Peskin and Schroeder [33].

For the B-type $\mathrm{SCET_{II}}$ operators (25), although naively the soft and collinear degrees of freedom seem to be decoupled, the factorization may be invalidated unless no end-point divergences appear in the convolution integrals [21, 22]. The relevant meson LCDAs are defined as [13, 34]

$$\begin{aligned}&\langle 0|\bar{\mathcal{Q}}_{\rm s}(tn)\Gamma\mathcal{H}_{\rm s}(0)|B(v)\rangle\\ &= \frac{\mathrm{i}F(\mu)}{2}\sqrt{m_B}\int_0^\infty \mathrm{d}\omega\,\mathrm{e}^{-\mathrm{i}\omega n\cdot vt}\\ &\quad\times\mathrm{tr}\left[\left(\phi^B_+(\omega,\mu) - \frac{\not n}{2n\cdot v}\big(\phi^B_-(\omega,\mu)-\phi^B_+(\omega,\mu)\big)\right)\right.\\ &\quad\left.\times\Gamma\mathcal{M}_B(v)\right],\\ &\big\langle K^*(p)|\bar{\mathcal{X}}_{\rm c}(s\bar n)\Gamma\frac{\not{\bar n}}{2}\mathcal{X}_{\rm c}(0)|0\big\rangle\\ &= \frac{\mathrm{i}f_{K^*}(\mu)}{4}\bar n\cdot p\,\mathrm{tr}\big[\overline{\mathcal{M}}_{K^*}\Gamma\big]\int_0^1\mathrm{d}u\,\mathrm{e}^{\mathrm{i}us\bar n\cdot p}\phi_{K^*}(u,\mu)\,,\end{aligned} \tag{36}$$

where two different K^*-distribution amplitudes ($\phi^\parallel_{K^*}(u,\mu)$ for $\Gamma = 1$ and $\phi^\perp_{K^*}(u,\mu)$ for $\Gamma = \gamma_\perp$) with their corresponding decay constants $f^\parallel_{K^*}$ and $f^\perp_{K^*}(\mu)$, respectively, are involved; $F(\mu)$ is related to the B meson decay constant f_B up to higher orders in $1/m_b$ by [35]

$$f_B\sqrt{m_B} = F(\mu)\left(1 + \frac{C_F\alpha_{\rm s}(\mu)}{4\pi}\left(3\ln\frac{m_b}{\mu} - 2\right)\right). \tag{37}$$

With the above LCDAs, the matrix elements of the operators O^B_i can be written as

$$\begin{aligned}&\big\langle K^*\ell^+\ell^-|C^B_1O^B_1|B\big\rangle\\ &= -\frac{F(\mu)m_B^{3/2}}{4}(1-\hat s)\big(g^{\mu\nu}_\perp - \mathrm{i}\epsilon^{\mu\nu}_\perp\big)\varepsilon^*_{\perp\nu}\bar\ell\gamma_\mu\ell\\ &\quad\times\int_0^\infty\frac{\mathrm{d}\omega}{\omega}\phi^B_+(\omega,\mu)\int_0^1\mathrm{d}u\,f_{K^*_\perp}(\mu)\phi_{K^*_\perp}(u,\mu)\\ &\quad\times\int_0^1\mathrm{d}v\mathcal{J}_\perp(u,v,\ln\frac{m_b\omega(1-\hat s)}{\mu^2},\mu)C^B_1(v,\mu)\\ &\equiv -\frac{F(\mu)m_B^{3/2}}{4}(1-\hat s)\big(g^{\mu\nu}_\perp - \mathrm{i}\epsilon^{\mu\nu}_\perp\big)\varepsilon^*_{\perp\nu}\bar\ell\gamma_\mu\ell\;\phi^B_+\\ &\quad\otimes f_{K^*_\perp}\phi_{K^*_\perp}\otimes\mathcal{J}_\perp\otimes C^B_1\,,\\ &\big\langle K^*\ell^+\ell^-|C^B_2O^B_2|B\big\rangle\\ &= -\frac{F(\mu)m_B^{3/2}}{4}(1-\hat s)\frac{n^\mu}{n\cdot v}\bar\ell\gamma_\mu\ell\;\phi^B_+\\ &\quad\otimes f_{K^*_\parallel}\phi_{K^*_\parallel}\otimes\mathcal{J}_\parallel\otimes C^B_2\,,\end{aligned} \tag{38}$$

while for the matrix element of $C^B_3O^B_3(C^B_4O^B_4)$, it can be obtained by simply replacing the lepton current $\bar\ell\gamma_\mu\ell$ on the right hand side of the above equations by $\bar\ell\gamma_\mu\gamma_5\ell$ and also replacing $C^B_1 \to C^B_3$ ($C^B_2 \to C^B_4$).

The matrix element of O^C is obtained likewise, with the result

$$\begin{aligned}\langle K^*\ell^+\ell^-|D^CO^C|B\rangle &= -\frac{F(\mu)m_B^{3/2}}{4}(1-\hat s)\frac{\bar n^\mu}{\bar n\cdot v}\bar\ell\gamma_\mu\ell\\ &\quad\times\frac{\omega\phi^B_-}{\omega - q^2/m_b - \mathrm{i}\epsilon}\otimes f_{K^*_\parallel}\phi_{K^*_\parallel}\otimes\widehat{D}^C\,.\end{aligned} \tag{39}$$

Since $\phi^B_-(\omega)$ does not vanish as ω approaches zero, the integral $\int\mathrm{d}\omega\;\phi^B_-(\omega)/(\omega - q^2/m_b)$ would be divergent if $q^2 \to 0$. This end-point singularity will violate the $\mathrm{SCET_{II}}$ factorization; that is why we should restrict our attention to the kinematic region where the invariant mass of the lepton pair is not too small, say $q^2 \geq 1\,\mathrm{GeV}^2$.

2.4 Resummation of logarithms in SCET

In the above analysis a two-step matching procedure $\mathrm{QCD} \to \mathrm{SCET_I} \to \mathrm{SCET_{II}}$ has been implemented. This introduces two matching scales, $\mu_h \sim m_b$ at which QCD is matched onto $\mathrm{SCET_I}$ and $\mu_l \sim \sqrt{m_b\Lambda}$ at which $\mathrm{SCET_I}$ is matched onto $\mathrm{SCET_{II}}$. Thus, with the $\mathrm{SCET_I}$ matching coefficients at scale μ_h, one may use the renormalization-group equations (RGE) of $\mathrm{SCET_I}$ to evolve them down to scale μ_l and then match onto $\mathrm{SCET_{II}}$. The large logarithms due to different scales are resummed during this procedure. Note that the meson LCDAs may be given at another scale μ_L, and, in principle, one should also use the RGE of $\mathrm{SCET_{II}}$ to run the corresponding matching coefficients from μ_l down to μ_L. But since in B decays the scale $\mu_l \simeq 1.5\,\mathrm{GeV}$ is already quite low, we may just take

the meson LCDAs at the scale μ_l in this paper for simplicity and thereby avoid the running of the $\mathrm{SCET_{II}}$ matching coefficients.

Furthermore, one should note that for the A-type SCET currents only the scale μ_h is involved, since it is not necessary to do the second step matching of $\mathrm{SCET_I} \to \mathrm{SCET_{II}}$. Similarly, we may choose the non-perturbative form factors $\zeta_{\perp,\parallel}$ at the scale μ_h and avoid the RGE running of the A-type $\mathrm{SCET_I}$ matching coefficients. For the B-type currents, the RGE of $\mathrm{SCET_I}$ can be obtained by calculating the anomalous dimensions of the relevant SCET operators, which has been done in [31], where the matching coefficients at any scale μ can be obtained by an evolution from the matching scale μ_h as follows:

$$\begin{aligned} &C_j^B(E,u,\mu_h,\mu) \\ &= \left(\frac{2E}{\mu_h}\right)^{a(\mu_h,\mu)} \mathrm{e}^{S(\mu_h,\mu)} \int_0^1 \mathrm{d}v\, U_\Gamma(u,v,\mu_h,\mu) C_j^B(E,v,\mu_h) \\ &\equiv \left(\frac{2E}{\mu_h}\right)^{a(\mu_h,\mu)} \mathrm{e}^{S(\mu_h,\mu)}\, \widetilde{U}_\Gamma^j(E,u,\mu_h,\mu)\,, \end{aligned} \tag{40}$$

with the subscript $\Gamma = \perp, \parallel$, and the functions $a(\mu_h,\mu)$ and $S(\mu_h,\mu)$ are given in (66) of [31]. Note that in the above equation one should use the subscript $\Gamma = \perp$ for $j = 1,3$ and $\Gamma = \parallel$ for $j = 2,4$. The evolution kernel $\widetilde{U}_\Gamma^j(E,u,\mu_h,\mu)$ obeys

$$\begin{aligned} \frac{\mathrm{d}\widetilde{U}_\Gamma^j(E,u,\mu_h,\mu)}{\mathrm{d}\ln\mu} &= \int_0^1 \mathrm{d}y\; y V_\Gamma(y,u) \widetilde{U}_\Gamma^j(E,y,\mu_h,\mu) \\ &\quad + \omega(u) \widetilde{U}_\Gamma^j(E,u,\mu_h,\mu)\,, \end{aligned} \tag{41}$$

with the initial condition $\widetilde{U}_\Gamma^j(E,u,\mu_h,\mu_h) = C_j^B(E,u,\mu_h)$. Again, the functions $V_\Gamma(y,u)$ and $\omega(u)$ are defined in [31]. In the next section on phenomenological application, we will solve the above integro-differential equation numerically.

Finally, for the C-type SCET current J^C, its anomalous dimension just equals the sum of the anomalous dimensions of the K^* meson LCDA ϕ_{K^*} and the B meson LCDA ϕ_-^B. However, as the evolution equation of ϕ_-^B is still unknown, we will not resum the perturbative logarithms for the J^C current in this paper. Numerically the contribution from the J^C current to the decay amplitude is small. Furthermore, as we will see later, the J^C current is completely irrelevant for the forward–backward asymmetry of the charged leptons. Therefore, this treatment has only a minor impact on our phenomenological discussion.

3 Numerical analysis of $B \to K^* \ell^+ \ell^-$

We are now in the position to write the decay amplitude of $B \to K^* \ell^+ \ell^-$, using a notation similar to the one adopted in [14],

$$\begin{aligned} \frac{\mathrm{d}^2\Gamma}{\mathrm{d}q^2 \mathrm{d}\cos\theta} &= \frac{G_\mathrm{F}^2 |V_{ts}^* V_{tb}|^2}{128\pi^3} \left(\frac{\alpha_\mathrm{em}}{4\pi}\right)^2 m_B^3 \lambda_{K^*} \left(1 - \frac{q^2}{m_B^2}\right)^2 \\ &\quad \times \Big\{ 2\zeta_\perp^2 (1+\cos^2\theta) \frac{q^2}{m_B^2} \left(|\mathcal{C}_9^\perp|^2 + (\mathcal{C}_{10}^\perp)^2\right) \\ &\quad - 8\zeta_\perp^2 \cos\theta \frac{q^2}{m_B^2} \mathrm{Re}\left(\mathcal{C}_9^\perp\right) \mathcal{C}_{10}^\perp \\ &\quad + \zeta_\parallel^2 (1-\cos^2\theta) \left(|\mathcal{C}_9^\parallel|^2 + (\mathcal{C}_{10}^\parallel)^2\right) \Big\}, \end{aligned} \tag{42}$$

with $m_B \lambda_{K^*}/2$ being the 3-momentum of the K^* meson in the rest frame of the B meson,

$$\lambda_{K^*} = \left[\left(1 - \frac{q^2}{m_B^2}\right)^2 - 2\frac{m_{K^*}^2}{m_B^2} \left(1 + \frac{q^2}{m_B^2}\right) + \frac{m_{K^*}^4}{m_B^4} \right]^{1/2}. \tag{43}$$

The angle θ denotes the angle between the momenta of the positively charged lepton and the B meson in the rest frame of the lepton pair. Note that in the above equations the leptons are taken in the massless limit and the K^* meson mass is kept non-zero only for λ_{K^*}, which arises from the phase space. The "effective" Wilson coefficients $\mathcal{C}_9^{\perp,\parallel}$ and $\mathcal{C}_{10}^{\perp,\parallel}$ are given by

$$\begin{aligned} \mathcal{C}_9^\perp &= \frac{2\pi}{\alpha_\mathrm{em}} \left(C_1^A + \frac{m_B}{4} \frac{f_B \phi_+^B \otimes f_{K^*}^\perp \phi_{K^*}^\perp \otimes \mathcal{J}_\perp \otimes C_1^B}{\zeta_\perp} \right), \\ \mathcal{C}_9^\parallel &= \frac{2\pi}{\alpha_\mathrm{em}} \left(C_2^A + \frac{m_B}{4} \frac{f_B \phi_+^B \otimes f_{K^*}^\parallel \phi_{K^*}^\parallel \otimes \mathcal{J}_\parallel \otimes C_2^B}{\zeta_\parallel} \right. \\ &\quad \left. - \frac{q^2}{4m_B} \frac{f_B \omega \phi_-^B / \left(\omega - q^2/m_b - \mathrm{i}\epsilon\right) \otimes f_{K^*}^\parallel \phi_{K^*}^\parallel \otimes \widehat{D}^C}{\zeta_\parallel} \right), \\ \mathcal{C}_{10}^\perp &= \frac{2\pi}{\alpha_\mathrm{em}} C_3^A\,, \\ \mathcal{C}_{10}^\parallel &= \frac{2\pi}{\alpha_\mathrm{em}} \left(C_4^A + \frac{m_B}{4} \frac{f_B \phi_+^B \otimes f_{K^*}^\parallel \phi_{K^*}^\parallel \otimes \mathcal{J}_\parallel \otimes C_4^B}{\zeta_\parallel} \right), \end{aligned} \tag{44}$$

where $C_i^{A,B}$ and D^C are defined in (13) and (32), respectively. The above expressions are valid at leading power in $1/m_b$ and to all orders in α_s. But in this paper we only calculate explicitly the "effective Wilson coefficients" at one-loop order. At this order our results are quite similar to those of [14] using the large-energy limit of QCD. The main phenomenological improvement is that for the hard scattering part; the matching coefficients C_i^B are evolved from the scale $\mu_h \sim \mathcal{O}(m_b)$ down to $\mu_l \sim \sqrt{m_b \Lambda_h}$, during which the perturbative logarithms are summed. Here, Λ_h represents a typical hadronic scale. Note also that the definitions of the soft form factors $\zeta_{\perp,\parallel}$ in SCET are different from those of [14]; therefore the explicit expressions for C_i^A are also different from the coefficients $C_a^{0,1}$ appearing in [14], which are related to the form factor corrections.

In terms of the helicity amplitudes for the decay $B \to K^*(\to K\pi)\ell^+\ell^-$, the double differential distribution $\mathrm{d}^2\mathcal{B}/\mathrm{d}\cos\theta_+ \mathrm{d}s$ is given in (44) of [36]. This requires the helicity amplitudes, $|H_0(s)|^2 = |H_0^L(s)|^2 + |H_0^R(s)|^2$,

$|H_-^{L,R}(s)|^2$ and $|H_+^{L,R}(s)|^2$. While the amplitudes $H_+^{L,R}(s)$ are both power-suppressed in $1/m_b$ and numerically small, the expressions for the other ones in SCET are given here:

$$|H_0|^2 = \frac{m_B^2}{2}\left(1-\frac{q^2}{m_B^2}\right)^2 \left(|\mathcal{C}_9^{\parallel}|^2 + (\mathcal{C}_{10}^{\parallel})^2\right)\zeta_{\parallel}^2\,,$$
$$|H_-^{L,R}|^2 = q^2\left(1-\frac{q^2}{m_B^2}\right)^2 |\mathcal{C}_9^{\perp} \pm \mathcal{C}_{10}^{\perp}|^2 \zeta_{\perp}^2\,. \quad (45)$$

Note that the dependence on the soft form factors factorizes in $\zeta_{\parallel}^2$ and $\zeta_{\perp}^2$ for the helicity components $|H_0|^2$ and $|H_-^{L,R}|^2$, respectively. Since a similar analysis in terms of the helicity amplitudes of the charged current decay $B \to \rho(\to \pi\pi)\ell^+\nu_\ell$ can be performed, the ratios $R_0(s)$ and $R_-(s)$ of the two differential distributions (in $B \to K^*(\to K\pi)\ell^+\ell^-$ and $B \to \rho(\to \pi\pi)\ell^+\nu_\ell$) have lot less hadronic uncertainties, as these ratios (see (76) in [36] for their definition) involve estimates of the $SU(3)$-breaking in the soft form factors. The point is that the ratios $\zeta_{\parallel}^{K^*}/\zeta_{\parallel}^{\rho}$ and $\zeta_{\perp}^{K^*}/\zeta_{\perp}^{\rho}$ are more reliably calculable than the form factors themselves.

3.1 Input parameters

To get the differential distributions numerically, some input parameters have to be specified. For the calculation of the Wilson coefficients, the relevant parameters are chosen as [37]

$$M_{\rm W} = 80.425\,{\rm GeV}\,, \quad \sin^2\theta_{\rm W} = 0.2312\,,$$
$$\Lambda_{\overline{\rm MS}}^{(5)} = 217^{+25}_{-23}\,{\rm MeV}\,, \quad (46)$$

and $m_t^{\rm pole} = (172.7 \pm 2.9)\,{\rm GeV}$, updated recently by the Tevatron electroweak group [38]. Numerical values of the Wilson coefficients, evaluated at scale $\mu = m_b = 4.8\,{\rm GeV}$, with the three-loop running of $\alpha_{\rm s}$ and the input parameters fixed at their central values given above are shown in Table 1. Note that the NNLL formula for C_9 can be found, for example, in the appendix of [14], while the relevant elements of the three-loop anomalous dimension matrix have been calculated recently in [39, 40].

The CKM factor $|V_{ts}V_{tb}^*| \simeq (1-\lambda^2/2)|V_{cb}|$ is estimated to be 0.0403 ± 0.0020 by taking $|V_{cb}| = 0.0413 \pm 0.0021$ [41] and $\lambda = 0.2226$. For the B meson lifetimes, we use $\tau_{B^+} = 1.643\,{\rm ps}$ and $\tau_{B^0} = 1.528\,{\rm ps}$ [41]. The pole mass m_b is chosen to be $4.8\,{\rm GeV}$. The ratio of the charm quark mass over the b-quark mass is taken to be $m_c/m_b = 0.29 \pm 0.02$. For the matching scale from ${\rm SCET_I}$ to ${\rm SCET_{II}}$, we use $\mu_l = \sqrt{m_b \Lambda_h} \simeq 1.5\,{\rm GeV}$.

The hadronic parameters for the decay $B \to K^*\ell^+\ell^-$ include decay constants, light-cone distribution amplitudes (LCDAs) and the soft form factors. The B meson decay constant can be estimated by QCD sum rules or lattice calculations; here we take $f_B = (200 \pm 30)\,{\rm MeV}$. For the K^* meson, experimental measurements give [37] $f_{K^*}^{\parallel} = (217 \pm 5)\,{\rm MeV}$, while the most recent light-cone sum rules (LCSRs) estimate [42] is $f_{K^*}^{\perp}(1\,{\rm GeV}) = (185 \pm 10)\,{\rm MeV}$. Note that $f_{K^*}^{\perp}$ obeys the scale evolution equation $f_{K^*}^{\perp}(\mu) = f_{K^*}^{\perp}(\mu_0)(\alpha_{\rm s}(\mu)/\alpha_{\rm s}(\mu_0))^{4/23}$.

The B meson LCDAs enter into the decay amplitudes only in terms of the integrated quantities $\lambda_{B,+}^{-1}$ and $\lambda_{B,-}^{-1}(q^2)$ defined by the following integrals:

$$\lambda_{B,+}^{-1} \equiv \int_0^\infty \frac{{\rm d}\omega}{\omega}\phi_+^B(\omega)\,,$$
$$\lambda_{B,-}^{-1}(q^2) \equiv \int_0^\infty {\rm d}\omega \frac{\phi_-^B(\omega)}{\omega - q^2/m_b - {\rm i}\epsilon}\,. \quad (47)$$

Therefore, it is not necessary to know the details about the shape of $\phi_+^B(\omega)$. The most recent estimate gives [43] $\lambda_{B,+}^{-1} = (1.86 \pm 0.34)\,{\rm GeV}^{-1}$ at the scale $\mu = 1.5\,{\rm GeV}$. However, $\lambda_{B,-}^{-1}(q^2)$ does require the knowledge of $\phi_-^B(\omega)$, about which we know very little. Fortunately, $\lambda_{B,-}^{-1}(q^2)$ only appears in the annihilation term which plays numerically a minor role in the $B \to K^*\ell^+\ell^-$ decay. To be definite, we adopt a simple model function [34], $\phi_-^B(\omega) = \omega_0^{-1}{\rm e}^{-\omega/\omega_0}$, with $\omega_0^{-1} \simeq 3\,{\rm GeV}^{-1}$.

The K^* meson LCDAs may be expanded in terms of Gegenbauer polynomials:

$$\phi_{K^*}^{\perp,\parallel}(u,\mu) = 6u(1-u)\left[1 + \sum_{n=1}^{\infty} a_n^{\perp,\parallel}(\mu) C_n^{3/2}(2u-1)\right]. \quad (48)$$

However, the coefficients a_n are largely unknown. Following [44], we shall ignore the terms $a_n^{\perp,\parallel}$ $(n > 2)$. For $a_{1,2}$, we omit their scale dependence and estimate in a conservative manner: $a_1^{\perp,\parallel} = 0.1 \pm 0.1$, $a_2^{\perp,\parallel} = 0.1 \pm 0.1$. We note that recently the first Gegenbauer moment of the K^* meson has been revisited in LCSRs [42], which gives smaller uncertainties.

There are only two independent $B \to K^*$ form factors in SCET, namely $\zeta_\perp(q^2)$ and $\zeta_\parallel(q^2)$. They are related to the full QCD form factors as discussed in [31]. The current knowledge of these form factors is fragmentary. For instance, $\zeta_\perp$ may be extracted from $V^{B\to K^*}$ [26]:

$$\zeta_\perp(q^2) = \frac{\zeta_\perp(0)}{r_1^V + r_2^V}\left(\frac{r_1^V}{1-q^2/m_V^2} + \frac{r_2^V}{1-q^2/m_{V\,\rm fit}^2}\right), \quad (49)$$

with $r_1^V = 0.923$, $r_2^V = -0.511$, $m_V = 5.32\,{\rm GeV}$ and $m_{V\,\rm fit}^2 = 49.40\,{\rm GeV}^2$. Note that the q^2-dependence above is the same as that of $V^{B\to K^*}(q^2)$, calculated in [44] using LCSRs. However, analyses of the radiative B decays $B \to K^*\gamma$ [14, 26, 45, 46], $B \to \rho\gamma$ [45, 46] and the semi-leptonic B decay $B \to \rho\ell\nu$ [47] imply that the LCSRs overestimate the $B \to V$ form factors significantly. We use the radiative $B \to K^*\gamma$ decay, which has been measured quite precisely [41]: $\mathcal{B}(B^0 \to K^{*0}\gamma) = (4.01 \pm 0.20) \times 10^{-5}$, to normalize the soft form factor at $q^2 = 0$. In SCET, it is straightforward to get the decay amplitude of $B \to K^*\gamma$ from the $B \to K_\perp^*\ell^+\ell^-$ decay, by taking the limit $q^2 \to 0$. Then, using the input parameters from Table 2, we obtain $\zeta_\perp(0) = 0.32 \pm 0.02$. Here the error is mainly from the CKM factor $V_{ts}V_{tb}^*$ and the experimental uncertainty of the

Table 2. Numerical values of the input parameters and their uncertainties used in the phenomenological study

M_W	80.425 GeV	$\sin^2\theta_W$	0.2312
$m_t^{\rm pole}$	(172.7 ± 2.9) GeV	$\Lambda^{(5)}_{\overline{\rm MS}}$	$\left(217^{+25}_{-23}\right)$ MeV
$\lvert V_{ts}V_{tb}^*\rvert$	$(40.3 \pm 2.0) \times 10^{-3}$	$\alpha_{\rm em}(m_{\rm b})$	1/133
m_B	5.279 GeV	$m_{\rm b}^{\rm pole}$	4.8 GeV
τ_{B^+}	1.643 ps	τ_{B^0}	1.528 ps
$m_c/m_{\rm b}$	0.29 ± 0.02	μ_l	1.5 GeV
$\lambda_{B,+}^{-1}(1.5\,{\rm GeV})$	(1.86 ± 0.34) GeV^{-1}	f_B	(200 ± 30) MeV
$\zeta_\perp(0)$	0.32 ± 0.02	$\zeta_\parallel(0)$	0.40 ± 0.05
$f_{K^*}^\perp(1\,{\rm GeV})$	(185 ± 10) MeV	$f_{K^*}^\parallel$	(217 ± 5) MeV
$a_1^{\perp,\parallel}$	0.1 ± 0.1	$a_2^{\perp,\parallel}$	0.1 ± 0.1

branching ratio $\mathcal{B}(B^0 \to K^{*0}\gamma)$. This estimate is consistent with the result of [26], but it is significantly smaller than the value of 0.40 ± 0.04 we get from LCSRs. In our numerical analysis, we will choose the value $\zeta_\perp(0) = 0.32 \pm 0.02$ as determined from the radiative B decays, but we assume that the q^2-dependence of $\zeta_\perp(q^2)$ can be reliably obtained from the LCSRs.

For the longitudinal soft form factor $\zeta_\parallel$, unfortunately, there is no quantitative determination from the existing experiments, though this may change in the future with good quality data available on the decay $B \to \rho \ell \nu_\ell$. Using a helicity analysis, one can extract $\zeta_\parallel^\rho(q^2)$; combined with estimates of the $SU(3)$-breaking one may determine $\zeta_\parallel^{K^*}(q^2)$. Not having this experimental information at hand, one may extract $\zeta_\parallel(q^2)$ from the full QCD form factor $A_0^{B\to K^*}(q^2)$:

$$
\begin{aligned}
&A_0^{B\to K^*}(q^2) \\
&= \left[1 - \frac{\alpha_{\rm s}(m_b) C_F}{4\pi}\left(2\ln^2[1-s] - \frac{2}{s}\ln[1-s]\right.\right. \\
&\quad \left.\left. + 2\,{\rm Li}_2[s] + 4 + \frac{\pi^2}{12}\right)\right]\zeta_\parallel(q^2) \\
&\quad - \frac{1}{4(1-s)} f_B \phi_+^B \otimes f_{K^*}^\parallel \phi_{K^*}^\parallel \otimes \mathcal{J}_\parallel \\
&\quad \otimes \left(\frac{2E}{\mu_h}\right)^{a(\mu_h,\mu_l)} {\rm e}^{S(\mu_h,\mu_l)} \int_0^1 {\rm d}y\, U_\parallel(v,y,\mu_h,\mu_l)\,,
\end{aligned}
\tag{50}
$$

with $s = q^2/m_B^2$. LCSRs estimate [44] $A_0^{B\to K^*}(0) = 0.374 \pm 0.043$ with the q^2-dependence

$$
A_0^{B\to K^*}(q^2) = \frac{1.364}{1 - q^2/m_B^2} - \frac{0.990}{1 - q^2/36.78{\rm GeV}^2}\,. \tag{51}
$$

From this we get $\zeta_\parallel(0) = 0.40 \pm 0.05$, using the input parameters discussed above and/or listed in Table 2. Its q^2-dependence is drawn in Fig. 4.

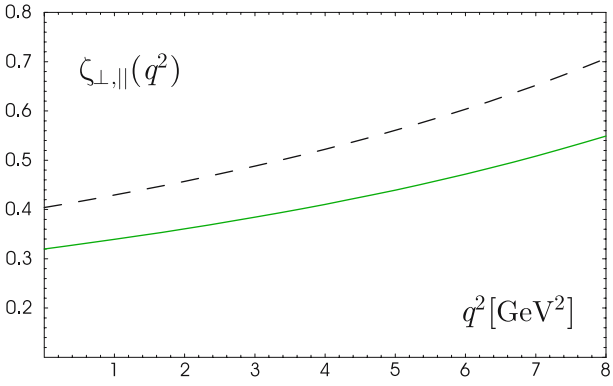

Fig. 4. The q^2-dependence of the soft form factors $\zeta_{\perp,\parallel}(q^2)$. The *solid curve* represents $\zeta_\perp(q^2)$, while the *dashed curve* represents $\zeta_\parallel(q^2)$. We have rescaled the transverse form factor at $q^2 = 0$ to be consistent with the experimental measurements of the $B \to K^*\gamma$ decay rate

Alternatively, $\zeta_\parallel(q^2)$ may also be determined from the following relation:

$$
\begin{aligned}
&\frac{E m_B (V - A_2)^{B\to K^*}(q^2)}{m_{K^*}(m_B + m_{K^*})} \\
&= \left[1 - \frac{\alpha_{\rm s}(m_b) C_F}{4\pi}\left(2\ln^2[1-s] - 2\ln[1-s]\right.\right. \\
&\quad \left.\left. + 2\,{\rm Li}_2[s] + 6 + \frac{\pi^2}{12}\right)\right]\zeta_\parallel(q^2) \\
&\quad - \frac{1-2s}{4(1-s)} f_B \phi_+^B \otimes f_{K^*}^\parallel \phi_{K^*}^\parallel \otimes \mathcal{J}_\parallel \otimes \left(\frac{2E}{\mu_h}\right)^{a(\mu_h,\mu_l)} \\
&\quad \times {\rm e}^{S(\mu_h,\mu_l)} \int_0^1 {\rm d}y\, U_\parallel(v,y,\mu_h,\mu_l)\,.
\end{aligned}
\tag{52}
$$

With the input $V^{B\to K^*}(0) - A_2^{B\to K^*}(0) = 0.152 \pm 0.057$ from LCSRs, we obtain $\zeta_\parallel(0) = 0.42 \pm 0.16$, which agrees with the range extracted from $A_0^{B\to K^*}$. We will use $\zeta_\parallel(0) = 0.40 \pm 0.05$, obtained from its relation to the full form factor $A_0^{B\to K^*}$ and the LCSR, as discussed above. Figure 4

shows the q^2-dependence of both soft form factors $\zeta_{\perp,\parallel}(q^2)$. However, since the analysis of the semileptonic decay $B \to \rho \ell \nu$ [47] suggests that both the transverse and longitudinal form factors might be overestimated by LCSRs, we will also consider, as an illustration of the non-perturbative uncertainties, the value $\zeta_\parallel(0) = \zeta_\perp(0) = 0.32$ with all the other parameters taken at their central values.

3.2 Numerical solution of the SCET$_\mathrm{I}$ evolution functions

As we discussed in Sect. 2.4, the B-type matching coefficients C_i^B should be run from the scale $\mu_h = 4.8\,\mathrm{GeV}$ down to $\mu_l = 1.5\,\mathrm{GeV}$, with the evolution kernel $\widetilde{U}_\Gamma(E, u, \mu_h, \mu)$ obeying the integro-differential equation (41). To solve this equation numerically, it is more convenient to define the following evolution functions:

$$\begin{aligned}
\widetilde{U}_\Gamma^{(a)}(E,u,\mu_h,\mu) &= \int_0^1 \mathrm{d}v U_\Gamma(u,v,\mu_h,\mu)\,,\\
\widetilde{U}_\Gamma^{(b)}(E,u,\mu_h,\mu) &= \frac{u+\hat{s}-u\hat{s}}{1-u}\int_0^1 \mathrm{d}v U_\Gamma(u,v,\mu_h,\mu)\\
&\quad\times\frac{1-v}{v+\hat{s}-v\hat{s}}\,,\\
\widetilde{U}_\Gamma^{(c)}(E,u,\mu_h,\mu) &= \int_0^1 \mathrm{d}v U_\Gamma(u,v,\mu_h,\mu)\frac{F_{16}^\Gamma\left(v,\hat{s},m_c^2/m_b^2\right)}{F_{16}^\Gamma\left(u,\hat{s},m_c^2/m_b^2\right)},
\end{aligned} \tag{53}$$

where $\Gamma = \perp, \parallel$, and the functions $F_{16}^{\perp,\parallel}(u,\hat{s},m_c^2/m_b^2)$ are defined in (18) and (19). Note that at the quark level the K^* meson energy is related to $\hat{s}$ by $E = m_b(1-\hat{s})/2$ in the rest frame of the b-quark. With such definitions, the above evolution functions are normalized to one at the scale μ_h: $\widetilde{U}_\Gamma^{(a,b,c)}(E,u,\mu_h,\mu_h) = 1$, and the QCD parameter $\Lambda_{\overline{\mathrm{MS}}}^{(5)}$ would be the only input for their numerical evaluations. The matching coefficients C_j^B at scale μ_l can then be written as

$$\begin{aligned}
\Delta_i C_j^B(E,u,\mu_l) &= \left(\frac{2E}{\mu_h}\right)^{a(\mu_h,\mu_l)} \mathrm{e}^{S(\mu_h,\mu_l)}\\
&\quad\times\widetilde{U}_\Gamma^{(a,b,c)}(E,u,\mu_h,\mu_l)\Delta_i C_j^B(E,u,\mu_h)\,,
\end{aligned} \tag{54}$$

where we should use the superscript (a) for $\Delta_{7,9,10}C_j^B$, the superscript (b) for $\Delta_8 C_j^B$ and the superscript (c) for $\Delta_{16}C_j^B$. For the subscript Γ, one should use $\Gamma = \perp$ for $j = 1,3$ and $\Gamma = \parallel$ for $j = 2,4$, which is the same as the convention of (40). Note that for the evolution of $\Delta_{16}C_j^B$, we have taken into account the fact that the term $F_{16}^\Gamma(u,\hat{s},m_c^2/m_b^2)$ is dominant due to the large Wilson coefficient $\bar{C}_2$.

It is then straightforward to get the following evolution equations:

$$\begin{aligned}
\frac{\mathrm{d}\widetilde{U}_\Gamma^{(a)}(E,u,\mu_h,\mu)}{\mathrm{d}\ln\mu} &= \int_0^1 \mathrm{d}y\, y V_\Gamma(y,u)\widetilde{U}_\Gamma^{(a)}(E,y,\mu_h,\mu)\\
&\quad+\omega(u)\widetilde{U}_\Gamma^{(a)}(E,u,\mu_h,\mu)\,,\\
\frac{\mathrm{d}\widetilde{U}_\Gamma^{(b)}(E,u,\mu_h,\mu)}{\mathrm{d}\ln\mu} &= \int_0^1 \mathrm{d}y\, y V_\Gamma(y,u)\frac{(1-y)(u+(1-u)\hat{s})}{(1-u)(y+(1-y)\hat{s})}\\
&\quad\times\widetilde{U}_\Gamma^{(b)}(E,y,\mu_h,\mu)\\
&\quad+\omega(u)\widetilde{U}_\Gamma^{(b)}(E,u,\mu_h,\mu)\,,
\end{aligned}$$

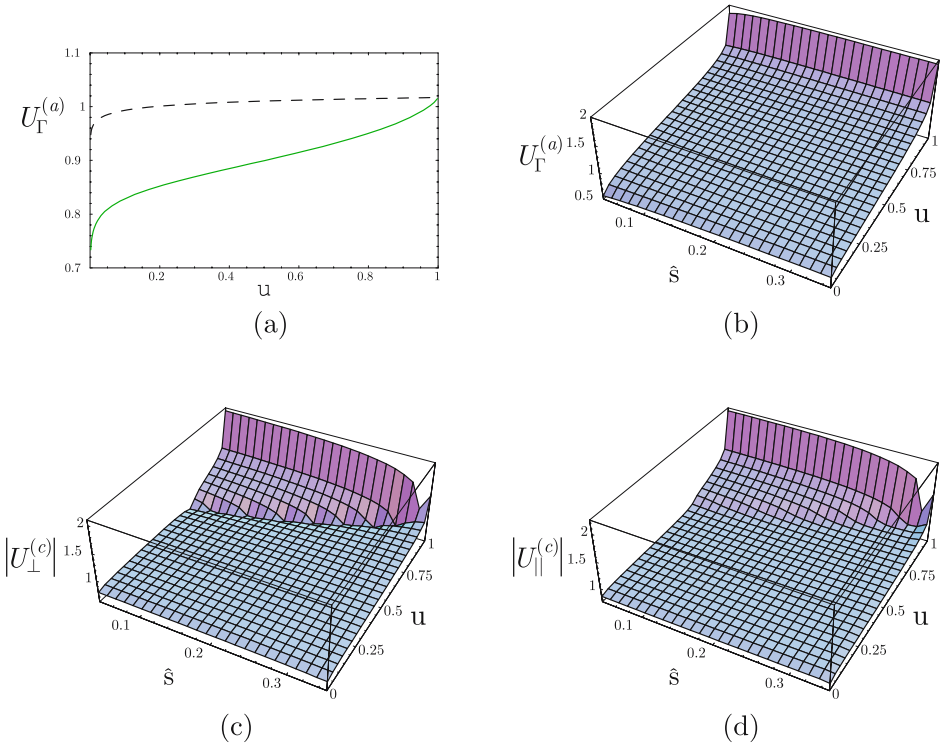

Fig. 5. Numerical values of the functions $\widetilde{U}_\Gamma^{(a,b,c)}(E,u,\mu_h,\mu_l)$, evolved from $\mu_h = 4.8\,\mathrm{GeV}$ down to $\mu_l = 1.5\,\mathrm{GeV}$; the relevant parameters are taken at their central values. For the upper-left plot, the *solid line* denotes $\widetilde{U}_\perp^{(a)}$, while the *dashed line* denotes $\widetilde{U}_\parallel^{(a)}$. For the lower plots, since $\widetilde{U}_\Gamma^{(c)}$ are complex functions, we only show their absolute values

$$\frac{\mathrm{d}\widetilde{U}_\Gamma^{(c)}(E,u,\mu_h,\mu)}{\mathrm{d}\ln\mu} = \int_0^1 \mathrm{d}y\, yV_\Gamma(y,u)\frac{F_{16}^\Gamma\left(y,\hat{s},m_c^2/m_b^2\right)}{F_{16}^\Gamma\left(u,\hat{s},m_c^2/m_b^2\right)} \times \widetilde{U}_\Gamma^{(c)}(E,y,\mu_h,\mu) + \omega(u)\widetilde{U}_\Gamma^{(c)}(E,u,\mu_h,\mu)\,. \quad (55)$$

To get the numerical solutions of the above integro-differential equations, we will perform the scale evolution in one hundred discrete steps, while from the scale μ_n to μ_{n+1}, the convolution integral is evaluated for three hundred different values and discrete $\hat{s}$-values of $\delta\hat{s} = 0.01$ in the interval $\hat{s} \in [0.04, 0.35]$. The function $\widetilde{U}_\Gamma(E,u,\mu_h,\mu_{n+1})$ is obtained from a fit to these values. Taking $\Lambda_{\overline{\rm MS}}^{(5)} = 217\,\mathrm{MeV}$, the numerical results of these evolution functions are shown in Fig. 5. Note that the function $\widetilde{U}_\Gamma^{(a)}(E,u,\mu_h,\mu)$ actually does not depend on the energy E, as shown in Fig. 5a. In fact, it is just the same function as $U_\Gamma(u,\mu_h,\mu)$ defined in (5.23) by Neubert et al. [31]. The function $\widetilde{U}_\parallel^{(b)}$ is not shown in Fig. 5, since it does not enter into the decay amplitude at the one-loop level, due to $\Delta_8 C_2^B = 0$. For the complex functions $\widetilde{U}_\Gamma^{(c)}$, only the absolute values of the functions are plotted.

3.3 The dilepton invariant mass spectrum and the forward–backward asymmetry

Experimentally, the dilepton invariant mass spectrum and the forward–backward (FB) asymmetry are the observables of principal interest. Their theoretical expressions in SCET can be easily derived from (42):

$$\frac{\mathrm{dBr}}{\mathrm{d}q^2} = \tau_B \frac{G_{\rm F}^2|V_{ts}^*V_{tb}|^2}{128\pi^3}\left(\frac{\alpha_{\rm em}}{4\pi}\right)^2 m_B^3|\lambda_{K^*}|\left(1-\frac{q^2}{m_B^2}\right)^2 \times\left\{\frac{16}{3}\zeta_\perp^2\frac{q^2}{m_B^2}\left(|\mathcal{C}_9^\perp|^2+\left(\mathcal{C}_{10}^\perp\right)^2\right)+\frac{4}{3}\zeta_\parallel^2\left(|\mathcal{C}_9^\parallel|^2+\left(\mathcal{C}_{10}^\parallel\right)^2\right)\right\}, \quad (56)$$

$$\frac{\mathrm{d}A_{FB}}{\mathrm{d}q^2} = \frac{1}{\mathrm{d}\Gamma/\mathrm{d}q^2}\left(\int_0^1 \mathrm{d}\cos\theta\frac{\mathrm{d}^2\Gamma}{\mathrm{d}q^2\mathrm{d}\cos\theta}-\int_{-1}^0 \mathrm{d}\cos\theta\frac{\mathrm{d}^2\Gamma}{\mathrm{d}q^2\mathrm{d}\cos\theta}\right) = \frac{-6\left(q^2/m_B^2\right)\zeta_\perp^2\,\mathrm{Re}\left(\mathcal{C}_9^\perp\right)\mathcal{C}_{10}^\perp}{4\left(q^2/m_B^2\right)\zeta_\perp^2\left(|\mathcal{C}_9^\perp|^2+(\mathcal{C}_{10}^\perp)^2\right)+\zeta_\parallel^2\left(|\mathcal{C}_9^\parallel|^2+(\mathcal{C}_{10}^\parallel)^2\right)}. \quad (57)$$

With the input parameters listed in Table 2, the decay spectrum and the FB asymmetry are shown in Figs. 6 and 7, respectively. In our calculation we have dropped the small isospin-breaking effects, which come from the annihilation diagrams, and we take the spectator quark as the down quark in (22) and (23). To estimate the residual scale dependence, we vary the QCD matching scale μ_h by a factor $\sqrt{2}$ around the default value $\mu_h = m_b$. Note that the soft form factors $\zeta_{\perp,\parallel}(q^2)$ defined in SCET are actually scale dependent, which effect has been taken into account in our error analysis.

Restricting ourselves to the integrated branching ratio of $B \to K^*\ell^+\ell^-$ in the range $1\,\mathrm{GeV}^2 \le q^2 \le 7\,\mathrm{GeV}^2$, where the SCET method should work, we obtain

$$\int_{1\,\mathrm{GeV}^2}^{7\,\mathrm{GeV}^2}\mathrm{d}q^2\frac{\mathrm{dBr}(B^+\to K^{*+}\ell^+\ell^-)}{\mathrm{d}q^2} = \left(2.92^{+0.57}_{-0.50}|_{\zeta_\parallel}{}^{+0.30}_{-0.28}|_{\rm CKM}{}^{+0.18}_{-0.20}\right)\times 10^{-7}\,. \quad (58)$$

Here we have isolated the uncertainties from the soft form factor $\zeta_\parallel$ and the CKM factor $|V_{ts}^*V_{tb}|$. The last error reflects the uncertainty due to the variation of the other input parameters and the residual scale dependence. If the smaller value for the longitudinal form factor $\zeta_\parallel(0) = 0.32$ is used, as shown in Fig. 6b, the central value of the branching ratio is reduced to 2.11×10^{-7}. For B^0 decay, the branching ratio is about 7% lower due to the lifetime difference:

$$\int_{1\,\mathrm{GeV}^2}^{7\,\mathrm{GeV}^2}\mathrm{d}q^2\frac{\mathrm{dBr}(B^0\to K^{*0}\ell^+\ell^-)}{\mathrm{d}q^2} = \left(2.72^{+0.53}_{-0.47}|_{\zeta_\parallel}{}^{+0.28}_{-0.26}|_{\rm CKM}{}^{+0.17}_{-0.19}\right)\times 10^{-7}\,. \quad (59)$$

To compare with the current experimental observations, it was proposed in [14] to consider the integrated branching ratio over the range $4\,\mathrm{GeV}^2 \le q^2 \le 6\,\mathrm{GeV}^2$, for which we get $(0.92^{+0.21}_{-0.19})\times 10^{-7}$. This is smaller than the number $(1.2\pm 0.4)\times 10^{-7}$ obtained in [14], which is mainly due to the fact that the most recent LCSRs estimation [44] favors smaller form factor $A_0^{B\to K^*}$. Experimentally one of the Belle observations [4] of our interest is

$$\int_{4\,\mathrm{GeV}^2}^{8\,\mathrm{GeV}^2}\mathrm{d}q^2\frac{\mathrm{dBr}(B\to K^*\ell^+\ell^-)}{\mathrm{d}q^2} = \left(4.8^{+1.4}_{-1.2}|_{\rm stat.}\pm 0.3|_{\rm syst.}\pm 0.3|_{\rm model}\right)\times 10^{-7}\,, \quad (60)$$

for which we predict $(1.94^{+0.44}_{-0.40})\times 10^{-7}$. This is smaller than the published Belle data by a factor of about 2.5. But at this stage, it is still too early to conclude that one should change some theoretical input significantly to be consistent with the experimental data. For instance, the BaBar collaboration measures the total branching ratio of $B \to K^*\ell^+\ell^-$ to be [3] $(7.8^{+1.9}_{-1.7}\pm 1.2)\times 10^{-7}$, which is about twice smaller than the Belle observation [4] $(16.5^{+2.3}_{-2.2}\pm 0.9\pm 0.4)\times 10^{-7}$. This implies that, if finally the total branching ratio of $B \to K^*\ell^+\ell^-$ is found to be closer to the BaBar result, the partially integrated branching ratio over the range $4\,\mathrm{GeV}^2 \le q^2 \le 8\,\mathrm{GeV}^2$ could be lowered to around 2.3×10^{-7}, which is consistent with our estimate $(1.94^{+0.44}_{-0.40})\times 10^{-7}$ within the stated errors. We look forward to experimental analyses from BaBar and Belle based on their high statistic data.

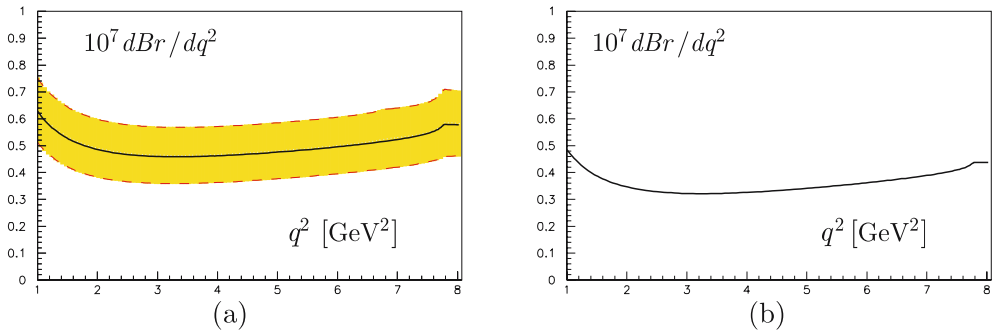

Fig. 6. The differential branching ratio $\mathrm{d}\mathcal{B}(B^0 \to K^{*0}\ell^+\ell^-)/\mathrm{d}q^2$ in the range $1\,\mathrm{GeV}^2 \le q^2 \le 8\,\mathrm{GeV}^2$. In the left plot, the *solid line* denotes the theoretical prediction with the input parameters taken at their central values, while the *gray area* between two *dashed lines* reflects the uncertainties from input parameters and scale dependence. In the right plot, the soft form factors are normalized as $\zeta_\parallel(0) = \zeta_\perp(0) = 0.32$, while all the other parameters are chosen at their central values

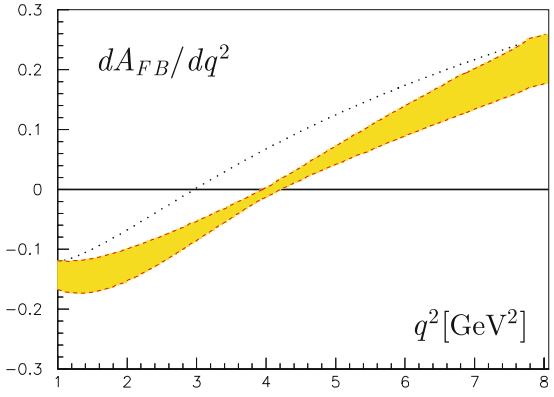

Fig. 7. The differential spectrum of the forward–backward asymmetry $\mathrm{d}A_{FB}(B \to K^*\ell^+\ell^-)/\mathrm{d}q^2$ in the range $1\,\mathrm{GeV}^2 \le q^2 \le 8\,\mathrm{GeV}^2$. Here the *solid line* denotes the theoretical prediction with the input parameters taken at their central values, while the *gray band* between two *dashed lines* reflects the uncertainties from input parameters and scale dependence. The *dotted line* represents the LO predictions, obtained by dropping the $O(\alpha_s)$ corrections

One of the most interesting observables in the decay $B \to K^*\ell^+\ell^-$ is the location, q_0^2, where the FB asymmetry vanishes. It was first noticed in the context of form factor models in [48] and later demonstrated in [12], using the symmetries of the effective theory in the large-energy limit, that the value of q_0^2 is almost free of hadronic uncertainties at leading order. From (57), it is easy to see that the location of the vanishing FB asymmetry is determined by $\mathrm{Re}(\mathcal{C}_9^\perp) = 0$. At the leading order, this leads to the equation $C_9 + C_7^{\mathrm{eff}} + \mathrm{Re}(Y(q_0^2)) = 0$. Including the order α_s corrections, our analysis estimates the zero-point of the FB asymmetry to be

$$q_0^2 = \left(4.07^{+0.16}_{-0.13}\right)\ \mathrm{GeV}^2\,, \qquad (61)$$

of which the scale-related uncertainty is $\Delta(q_0^2)_{\mathrm{scale}} = ^{+0.08}_{-0.05}$ GeV^2 for the range $m_b/2 \le \mu_h \le 2m_b$ together with the jet function scale $\mu_l = \sqrt{\mu_h \times 0.5\,\mathrm{GeV}}$, as used in the paper by Beneke et al. [14]. Since no reliable estimates of the power corrections in $1/m_b$ are available, we should compare our results with the one given in (74) of [14], also obtained in the absence of $1/m_b$ corrections: $q_0^2 = (4.39^{+0.38}_{-0.35})\ \mathrm{GeV}^2$. Of this the largest single uncertainty (about $\pm 0.25\,\mathrm{GeV}^2$) is attributed to the scale dependence. While our central value for q_0^2 is similar to theirs, with the differences reflecting the different input values, the scale dependence in our analysis is significantly smaller than that of [14]. This improved theoretical precision on q_0^2 requires a detailed discussion on which we now concentrate in the rest of this section.

As already stated in the introduction, the expressions for the differential distributions in the decay $B \to K^*\ell^+\ell^-$ derived here and in [14] are similar except for the definitions of the soft form factors and the additional step of the SCET logarithmic resummation incorporated in our paper. This resummation has also been derived in the existing literature [26, 31, 49]. However, its effect on the scale dependence of q_0^2 has not been studied in sufficient detail. With the SCET form factors $\zeta_\perp(q^2, \mu)$ and $\zeta_\parallel(q^2, \mu)$ defined in (33) here, which are scale-dependent quantities, and neglecting the resummation effects consistently in both the decays $B \to K^*\ell^+\ell^-$ and $B \to K^*\gamma$, the scale uncertainty is increased, with $q_0^2 = 4.12^{+0.17}_{-0.07}\,\mathrm{GeV}^2$. We draw two inferences from this numerical study, (i) Incorporating the SCET logarithmic resummation helps in the reduction of scale dependence in q_0^2. (ii) $\Delta(q_0^2)_{\mathrm{scale}} = ^{+0.17}_{-0.07}$ GeV^2, obtained by dropping the resummation effects, is still significantly smaller (by a factor 2) compared to the corresponding uncertainty $\Delta(q_0^2)_{\mathrm{scale}} = \pm 0.25\,\mathrm{GeV}^2$ calculated in [14]. This difference, as argued below, is to be traced back to the different definitions of the soft form factors used by us for the SCET currents and the corresponding quantities employed by Beneke et al. [14] in the QCD factorization approach. The results in [14] are, however, formally equivalent to the so-called "physical form factor" (PFF) scheme in SCET, as discussed subsequently by Beneke and Yang [49]. Thus, the scale dependence of the distributions in $B \to K^*\ell^+\ell^-$, in particular of q_0^2, is related also to the definitions (or scheme dependence) of the form factors in effective theories. The PFF scheme is one such choice, but this choice is by no means unique.

Concentrating on the transverse form factor, relevant for q_0^2 of the FB asymmetry, in the PFF scheme, the corresponding $\mathrm{SCET_I}$ form factor $\zeta_\perp^P$ (where we have now added a superscript P for this scheme) is defined as

$$\zeta_\perp^P \equiv \frac{m_B}{m_B + m_{K^*}} V \,, \tag{62}$$

where V is one of the physical form factors in the decay $B \to K^* \ell^+ \ell^-$ in full QCD. In contrast, in our paper, the soft SCET form factors are defined in (33). These two definitions can be related to each other by $\zeta_\perp^P = \widetilde{C}_3 \zeta_\perp$, where the expression for the perturbative QCD coefficient $\widetilde{C}_3$ is given below ($\widetilde{C}_3$ is called $C_V^{(A0)1}$ in [23]). Since the decay amplitude should be independent on how one defines the soft form factors, one must have

$$\mathcal{C}_9^{\perp P} \zeta_\perp^P \equiv \mathcal{C}_9^\perp \zeta_\perp \Longrightarrow \mathcal{C}_9^{\perp P} = \mathcal{C}_9^\perp / \widetilde{C}_3 \,. \tag{63}$$

Since $\widetilde{C}_3 = 1 + \mathcal{O}(\alpha_\mathrm{s})$, by expanding $\mathcal{C}_9^\perp / \widetilde{C}_3$ to order α_s, one obtains

$$\begin{aligned}
&\mathcal{C}_9^{\perp P} \\
&= \frac{\mathcal{C}_9^\perp}{1 - (1 - \widetilde{C}_3)} \simeq \frac{2\pi}{\alpha_\mathrm{em}} \Bigg(C_1^A + \frac{\alpha_\mathrm{em}}{2\pi} (1 - \widetilde{C}_3) \left(\frac{2}{\hat{s}} C_7^\mathrm{eff} + C_9^\mathrm{eff} \right) \\
&\quad + \frac{m_B}{4} \frac{f_B \phi_+^B \otimes f_{K^*}^\perp \phi_{K^*}^\perp \otimes \mathcal{J}_\perp \otimes C_1^B}{\zeta_\perp^P} \Bigg) \\
&= C_9^\mathrm{eff} \\
&\quad + \frac{2}{\hat{s}} C_7^\mathrm{eff} \left(1 + \frac{C_F \alpha_\mathrm{s}}{4\pi} \left[4 \ln \frac{m_b^2}{\mu^2} - 4 + \frac{1 - \hat{s}}{\hat{s}} \ln(1 - \hat{s}) \right] \right) + \ldots \,,
\end{aligned} \tag{64}$$

which agrees with the expression for $\mathcal{C}_9^{\perp P}$ in (40) of [14] (called $C_{9,\perp}(q^2)$ there). We recall that to determine q_0^2, we solve the equation $\mathrm{Re}\, \mathcal{C}_9^\perp = 0$, where now the quantity $\mathcal{C}_9^\perp$ is defined as follows:

$$\mathcal{C}_9^\perp = \widetilde{C}_3(\mu) C_9^\mathrm{eff} + \frac{2}{\hat{s}} C_7^\mathrm{eff} \frac{\overline{m}_b}{m_b} \widetilde{C}_9(\mu) + \ldots \,, \tag{65}$$

with the QCD coefficients [16] ($\widetilde{C}_9$ is called $C_T^{(A0)2}$ in [23])

$$\begin{aligned}
\widetilde{C}_3 &= 1 - \frac{\alpha_\mathrm{s} C_F}{4\pi} \left[2 \ln^2 \left(\frac{\mu}{m_b} \right) - (4 \ln(1 - \hat{s}) - 5) \ln \left(\frac{\mu}{m_b} \right) \right. \\
&\quad \left. + 2 \ln^2(1 - \hat{s}) + 2 \mathrm{Li}_2(\hat{s}) + \frac{\pi^2}{12} + \left(\frac{1}{\hat{s}} - 3 \right) \ln(1 - \hat{s}) + 6 \right] , \\
\widetilde{C}_9 &= 1 - \frac{\alpha_\mathrm{s} C_F}{4\pi} \left[2 \ln^2 \left(\frac{\mu}{m_b} \right) - (4 \ln(1 - \hat{s}) - 7) \ln \left(\frac{\mu}{m_b} \right) \right. \\
&\quad \left. + 2 \ln^2(1 - \hat{s}) - 2 \ln(1 - \hat{s}) + 2 \mathrm{Li}_2(\hat{s}) + \frac{\pi^2}{12} + 6 \right] .
\end{aligned} \tag{66}$$

The ellipsis above denotes the terms which are the same for $\mathcal{C}_9^{\perp P}$ and $\mathcal{C}_9^\perp$. The functions multiplying the effective Wilson coefficients C_9^eff and C_7^eff appearing in $\mathcal{C}_9^{\perp P}$ and $\mathcal{C}_9^\perp$ in (64) and (65), respectively, lead to a different scale dependence for q_0^2.

Our result for q_0^2 using the SCET form factors has been given above in (61) with the scale-dependent uncertainty $\Delta(q_0^2)_\mathrm{scale} = ^{+0.08}_{-0.05}\ \mathrm{GeV}^2$. Note that we have considered in a correlated way the scale dependence of $\zeta_\perp(\mu, q^2)$ in our analysis. To illustrate this, we use the experimental data on the branching ratio of $B \to K^* \gamma$ and the central values of the other input parameters given in Table 2, which yields the following scale dependence of the relevant form factor: $\zeta_\perp(0, \mu = 2m_b) = 0.34$ and $\zeta_\perp(0, \mu = m_b/2) = 0.30$. In solving the equation $\mathrm{Re}[\mathcal{C}_9^\perp] = 0$, relevant for the zero-point of the FB asymmetry in the decay $B \to K^* \ell^+ \ell^-$, we have factored in the scale dependence of $\zeta_\perp(\mu, q^2)$. We do a similar numerical analysis of q_0^2 in the PFF scheme, where the corresponding form factor $\zeta_\perp^P(q^2)$ is scale-independent, and we incorporate the effect of the logarithmic resummation in both the $B \to K^* \gamma$ and $B \to K^* \ell^+ \ell^-$ decays. Solving now the equation $\mathrm{Re}[\mathcal{C}_9^{\perp P}] = 0$, using the central value of the soft form factor $\zeta_\perp^P(0)$ obtained from the analysis of the $B \to K^* \gamma$ branching ratio, $\zeta_\perp^P(0) = 0.28$, and with all the other parameters fixed at their central values given in Table 2, we find that in the PFF scheme $q_0^2 = 3.98 \pm 0.18\ \mathrm{GeV}^2$. Had we dropped the resummation effect, we would get $q_0^2 = 4.03 \pm 0.22\ \mathrm{GeV}^2$, where the scale uncertainty $\Delta(q_0^2)_\mathrm{scale} = \pm 0.22\ \mathrm{GeV}^2$, derived here in the PFF scheme, is consistent with the number $\Delta(q_0^2)_\mathrm{scale} = \pm 0.25\ \mathrm{GeV}^2$ obtained in [14]. Therefore, we conclude that the difference in the estimates of the scale dependence of q_0^2 here and in [14] is both due to the incorporation of the SCET logarithmic resummation and the different (scheme-dependent) definitions of the effective form factors for the SCET currents and the ones used by Beneke et al. [14]. Using the SCET form factors defined in (33) in this paper, we find that the scale-related uncertainty $\Delta(q_0^2)_\mathrm{scale}$ is reduced compared to the PFF scheme of Beneke et al. [14]. One expects that such scheme-dependent differences will become less marked after incorporating the $O(\alpha_\mathrm{s}^2)$ effects in the decay distributions for $B \to K^* \ell^+ \ell^-$. Our comparative analysis hints at rather large $O(\alpha_\mathrm{s}^2)$ corrections to q_0^2 in the PFF scheme and a moderate correction in the SCET analysis carried out by us in this paper. Since the value of q_0^2 offers a precision test of the SM, and by that token it provides a window on the possible beyond-the-SM physics effects; it is mandatory to undertake an $O(\alpha_\mathrm{s}^2)$ improvement of the current theory of $B \to K^* \ell^+ \ell^-$ decay. As power corrections in $1/m_b$ have not been considered here, although they are probably comparable to the $O(\alpha_\mathrm{s})$ corrections as argued in a model-dependent estimate of the $1/m_b$ corrections by Beneke et al. [14], it also remains to be seen how a model-independent calculation of the same affects the numerical value of q_0^2.

4 Summary

In this paper, we have examined the rare B decay channel $B \to K^* \ell^+ \ell^-$ in the framework of SCET, where the factorization formula holds to all orders in α_s and leading order in $1/m_b$. Making use of the existing literature, we work with the relevant effective operators in SCET,

and the corresponding matching procedures are discussed in detail. The logarithms related to the different scales $\mu_h = m_b$ and $\mu_l = \sqrt{m_b \Lambda_h}$ are resummed by solving numerically the renormalization-group equation in SCET. We then give explicit expressions for the differential distributions in q^2 for the decay $B \to K^* \ell^+ \ell^-$ including the $O(\alpha_s)$ corrections. In the phenomenological analysis, we first discuss the input parameters, especially how to extract the soft form factors $\zeta_{\perp,\parallel}(q^2)$ from the full QCD form factors, and also the constraints on $\zeta_\perp(0)$ from the experimental data on the $B \to K^* \gamma$ decay. Using the q^2-dependence of the form factors from the LCSRs and the normalization $\zeta_\perp(0) = 0.32 \pm 0.02$ and $\zeta_\parallel(0) = 0.40 \pm 0.05$, we work out the differential branching ratio and the forward–backward asymmetry as a function of the dilepton invariant mass. In the region $1\ \mathrm{GeV}^2 \le q^2 \le 7\ \mathrm{GeV}^2$, where the perturbative method should be reliable, our analysis yields

$$\int\limits_{1\ \mathrm{GeV}^2}^{7\ \mathrm{GeV}^2} \mathrm{d}q^2 \frac{\mathrm{dBr}(B^+ \to K^{*+} \ell^+ \ell^-)}{\mathrm{d}q^2} = \left(2.92^{+0.67}_{-0.61}\right) \times 10^{-7}\,, \tag{67}$$

which can be compared with the B factory measurements in the near future. The largest uncertainty in the branching ratio is due to the imprecise knowledge of $\zeta_\parallel(q^2)$. We have illustrated this by using the value $\zeta_\parallel(0) = 0.32$, which reduces the central value of the branching ratio to 2.11×10^{-7}. We point out that precisely measured q^2-distributions in $B \to K^* \ell^+ \ell^-$ and $B \to \rho \ell \nu_\ell$ would greatly reduce the form factor related uncertainties in the differential branching ratios. The FBA is less dependent on the soft form factors, and the residual parametric dependencies are worked out. We estimate the zero-point of the FBA to be $q_0^2 = (4.07^{+0.16}_{-0.13})\ \mathrm{GeV}^2$. The stability of this result against $O(\alpha_s^2)$ and $1/m_b$ corrections should be investigated in the future.

Acknowledgements. G.Z. acknowledges the financial support from Alexander-von-Humboldt Stiftung. G.Z. is also grateful to D.S. Yang for useful discussions. We thank Martin Beneke, Thorsten Feldmann, Alexander Parkhomenko and Dan Pirjol for their comments on the earlier version of this manuscript and helpful communications.

References

1. Belle Collaboration, J. Kaneko et al., Phys. Rev. Lett. **90**, 021 801 (2003) [hep-ex/0208029]
2. BABAR Collaboration, B. Aubert et al., Phys. Rev. Lett. **93**, 081 802 (2004) [hep-ex/0404006]
3. BaBar Collaboration, B. Aubert et al., hep-ex/0507005, contributed to 22nd International Symposium on Lepton–Photon Interactions at High Energy (LP 2005), Uppsala, Sweden, 30 June–5 July 2005
4. Belle Collaboration, K. Abe et al., hep-ex/0410006, presented at 32nd International Conference on High-Energy Physics (ICHEP 04), Beijing, China, 16–22 August 2004
5. Belle Collaboration, K. Abe et al., hep-ex/0508009
6. A. Ali, T. Mannel, T. Morozumi, Phys. Lett. B **273**, 505 (1991)
7. N.G. Deshpande, J. Trampetic, K. Panose, Phys. Rev. D **39**, 1461 (1989)
8. C.S. Lim, T. Morozumi, A.I. Sanda, Phys. Lett. B **218**, 343 (1989)
9. A. Ali, T. Mannel, Phys. Lett. B **264**, 447 (1991) [Erratum-ibid. B **274**, 526 (1992)]
10. C. Greub, A. Ioannisian, D. Wyler, Phys. Lett. B **346**, 149 (1994)
11. D. Melikhov, N. Nikitin, S. Simula, Phys. Lett. B **410**, 290 (1997)
12. A. Ali, P. Ball, L.T. Handoko, G. Hiller, Phys. Rev. D **61**, 074 024 (2000) [hep-ph/9910221]
13. M. Beneke, G. Buchalla, M. Neubert, C.T. Sachrajda, Phys. Rev. Lett. **83**, 1914 (1999); Nucl. Phys. B **591**, 313 (2000)
14. M. Beneke, T. Feldmann, D. Seidel, Nucl. Phys. B **612**, 25 (2001); Eur. Phys. J. C **41**, 173 (2005)
15. C.W. Bauer, S. Fleming, M.E. Luke, Phys. Rev. D **63**, 014 006 (2001)
16. C.W. Bauer, S. Fleming, D. Pirjol, I.W. Stewart, Phys. Rev. D **63**, 114 020 (2001)
17. C.W. Bauer, I.W. Stewart, Phys. Lett. B **516**, 134 (2001)
18. M. Beneke, A.P. Chapovsky, M. Diehl, T. Feldmann, Nucl. Phys. B **643**, 431 (2002)
19. R.J. Hill, M. Neubert, Nucl. Phys. B **657**, 229 (2003)
20. C.W. Bauer, D. Pirjol, I.W. Stewart, Phys. Rev. D **65**, 054 022 (2002) [hep-ph/0109045]
21. B. Lange, M. Neubert, Nucl. Phys. B **690**, 249 (2004); [Erratum-ibid. B **723**, 201 (2005)]
22. M. Beneke, T. Feldmann, Nucl. Phys. B **685**, 249 (2004); Eur. Phys. J. C **33**, 241 (2004)
23. M. Beneke, Y. Kiyo, D.S. Yang, Nucl. Phys. B **692**, 232 (2004)
24. D. Pirjol, I.W. Stewart, Phys. Rev. D **67**, 094 005 (2003) [Erratum-ibid. D **69**, 019 903 (2004)] [hep-ph/0211251]
25. C.W. Bauer, D. Pirjol, I.W. Stewart, Phys. Rev. D **67**, 071 502 (2003) [hep-ph/0211069]
26. T. Becher, R.J. Hill, M. Neubert, Phys. Rev. D **72**, 094 017 (2005)
27. J.g. Chay, C. Kim, Phys. Rev. D **68**, 034 013 (2003)
28. B. Grinstein, D. Pirjol, hep-ph/0505155
29. F. Krüger, L.M. Sehgal, Phys. Lett. B **380**, 199 (1996)
30. K. Chetyrkin, M. Misiak, M. Münz, Phys. Lett. B **400**, 206 (1997)
31. R.J. Hill, T. Becher, S.J. Lee, M. Neubert, JHEP **0407**, 081 (2004)
32. H.H. Asatryan, H.M. Asatrian, C. Greub, M. Walker, Phys. Lett. B **507**, 162 (2001); Phys. Rev. D **65**, 074 004 (2002)
33. M.E. Peskin, D.V. Schroeder, An Introduction to Quantum Field Theory (Addison-Wesley, Reading, MA, USA, 1995)
34. A.G. Grozin, M. Neubert, Phys. Rev. D **55**, 272 (1997)
35. M. Neubert, Phys. Rept. **245**, 259 (1994)
36. A. Ali, A.S. Safir, Eur. Phys. J. C **25**, 583 (2002) [hep-ph/0205254]
37. Particle Data Group, S. Eidelman et al., Phys. Lett. B **592**, 1 (2004)
38. CDF Collaboration, D0 Collaboration and the Tevatron Electroweak Working Group, hep-ex/0507091
39. P. Gambino, M. Gorbahn, U. Haisch, Nucl. Phys. B **673**, 238 (2003)

40. M. Gorbahn, U. Haisch, Nucl. Phys. B **713**, 291 (2005)
41. The Heavy Flavor Averaging Group, http://www.slac.stanford.edu/xorg/hfag/ (Winter 2005 averages)
42. P. Ball, R. Zwicky, Phys. Lett. B **633**, 289 (2006) [hep-ph/0510338]
43. S.J. Lee, M. Neubert, Phys. Rev. D **72**, 094 028 (2005)
44. P. Ball, R. Zwicky, Phys. Rev. D **71**, 014 029 (2005)
45. A. Ali, A.Y. Parkhomenko, Eur. Phys. J. C **23**, 89 (2002) [hep-ph/0105302]; Phys. Lett. B **595**, 323 (2004) [hep-ph/0405075]
46. S.W. Bosch, G. Buchalla, Nucl. Phys. B **621**, 459 (2002)
47. BABAR Collaboration, B. Aubert et al., hep-ex/0507003
48. G. Burdman, Phys. Rev. D **57**, 4254 (1998)
49. M. Beneke, D. Yang, Nucl. Phys. B **736**, 34 (2006) [hep-ph/0508250]